N-Glycans on the extracellular domain of the Notch1 receptor control Jagged-1 induced Notch signalling and myogenic differentiation of S100β resident vascular stem cells

Eoin Corcoran[1], Abidemi Olayinka[1], Mariana di Luca[1], Yusof Gusti[1],
Roya Hakimjavadi[1], Brendan O'Connor[2], Eileen M. Redmond[3] and Paul A. Cahill[1]*

[1] Vascular Biology and Therapeutics Laboratory, School of Biotechnology Faculty of Science and Health, Dublin City University, Dublin, Ireland.

[2] School of Biotechnology Faculty of Science and Health, Dublin City University, Dublin, Ireland

[3] Department of Surgery, University of Rochester, 601 Elmwood Ave, Rochester, NY 14642, United States

Abstract

Notch signalling, critical for development and postnatal homeostasis of the vascular system, is highly regulated by several mechanisms including glycosylation. While the importance of O-linked glycosylation is widely accepted, the structure and function of N-glycans has yet to be defined. Here, we take advantage of lectin binding assays in combination with pharmacological, molecular, and site-directed mutagenetic approaches to study N-glycosylation of the Notch1 receptor. We find that several key oligosaccharides containing bisecting or core fucosylated structures decorate the receptor, control expression and receptor trafficking, and dictate Jagged-1 activation of Notch target genes and myogenic differentiation of multipotent S100β vascular stem cells. N-glycans at asparagine (N) 1241 and 1587 protect the receptor from accelerated degradation, while the oligosaccharide at N888 directly affects signal transduction. Conversely, N-linked glycans at N959, N1179, N1489 do not impact canonical signalling but inhibit differentiation. Our work highlights a novel functional role for N-glycans in controlling Notch1 signalling and differentiation of vascular stem cells.

Short title

A sweet development in Notch regulation of vascular smooth muscle cell differentiation

Introduction

The Notch signalling pathways is crucial for the development and postnatal homeostasis of the vascular system[1] . It is activated by interaction of receptors (Notch1–4) and ligands (Delta-like 1, 3, 4, and Jagged 1, 2) present on the surface of adjacent cells [2]. This interaction triggers sequential

cleavage events resulting in release of the active form of Notch i.e., Notch intracellular domain (NICD). NICD translocates into the nucleus and, in combination with the transcription factor recombinant binding protein for the immunoglobulin region kJ (RBPJ, also known as CBF1/Suppressor of Hairless/LAG1, CSL) and the Mastermind-like (MAML 1–3) adaptor proteins, activates target genes including HES (Hairy and Enhancer of Split) and HEY (Hairy/enhancer-of-split related) that are essential modulators of neuronal, endocrine, and cardiovascular cell fate [3]. The Notch pathway may also be activated in the absence of 'canonical' ligands and independent of γ-secretase proteolytic cleavage; this non-canonical Notch signalling modulates Wnt/β-catenin, mammalian target of the rapamycin 2 complex (mTORC2)/Akt, Nuclear Factor kappa B (NF-κB), IkB kinase (IKK)-α/β and phosphatase and tensin homolog (PTEN)-induced kinase (PINK1)[4].

There is now compelling evidence from several lineage tracing studies for the involvement of (i) a rare subpopulation of differentiated medial vascular smooth muscle cells (SMC) that are stem cell antigen-1 (Sca1) positive [5,6] and (ii) various adventitial [7,8] and medial progenitors [9–14] in progressing subclinical atherosclerosis through the accumulation of 'SMC-like' cells within the vessel wall. Notch significantly impacts arterial pathology during lesion development [15–19] by promoting SMC-like cell accumulation after injury [19,20]. Multiple studies describe the ability of Notch signalling to induce myogenic differentiation of stem cell populations such as C3H 10T1/2 embryonic fibroblasts, mesenchymal stromal stem cells and neural crest stem cells [21–23]. While the exact mechanism and cell(s) involved by which Notch and its target genes affect lesion formation remains incompletely understood, there is substantial evidence suggesting that the Notch1 receptor in particular plays a pivotal role in this process [17,19,20].

The Notch signalling pathway is tightly regulated by several mechanisms including cis-inhibition, negative feedback loops and PEST ubiquitination [24,25] and by glycosylation of the Notch receptor [26]. There are several highly conserved glycosylation sites along the extracellular domain of the Notch receptor, most of which harbour O-linked glycans [27–29]. In contrast, very little is known about the specifics of N-linked glycosylation of Notch. It has been established that there are six N-glycosylation consensus sites along the extracellular domain of Notch [30] and that N-glycans are certainly present on the Notch receptor [31] but the number of these sites that are glycosylated, the structures of these N-glycans and their potential role in Notch signalling, remains unknown.

The impact of N-glycan decoration of key proteins on a given process can be revealed using chemical inhibitors of N-glycosylation. Tunicamycin (TNC), an antagonist for the GlcNAc phosphotransferase (GPT) enzyme, catalyses a critical step in the protein N-glycosylation pathway, linking the growing polypeptide to a dolichol precursor [32]. 1-deoxymannojirimycin (DMJ) blocks the trimming of the 14-sugar dolichol precursor oligosaccharide by inhibiting the mannosidase I enzyme and preventing the synthesis of complex or hybrid-type N-glycans [33]. Because the specificities of these inhibitors are broad, a more targeted approach for regulating N-glycans can be achieved using siRNA knockdown of key glycosyltransferases, Fut8 and Mgat3. A family of glycosyltransferases known as N-acetylglucosaminyl transferases (GnT's) are responsible for the addition of GlcNAc residues to N-linked glycans. There are six members of this family (GnT-I to GnT-VI), all of which operate in the Golgi apparatus [34]. GnT-III (coded by the *Mgat3* gene) catalyses the addition of a GlcNAc residue through a β-1,4 linkage to the β-mannose in the tri-mannosyl core of a growing N-linked oligosaccharide, creating a structure known as a bisecting N-glycan [35]. This structure has been shown to inhibit the addition of sugar residues by other glycosyltransferases such as GnT-II, GnT-IV and Fut8 [36,37]. Bisecting N-glycans are heavily involved in the regulation of several cellular processes, including cell adhesion, protein degradation and growth factor signalling [38]. Members of the fucosyltransferase (FUT)

family of enzymes facilitate the addition of fucose residues to the core N-glycan structure in a process known as core fucosylation [39]. Fut8 catalyses the transfer of fucose from a donor substrate to the asparagine-149 bound GlcNAc at the base of an N-glycan via an α1,6-linkage [40]. Core-fucosylated N-glycans regulate a wide array of cellular processes such as the expression of essential cadherins and the function of specific types of immunoglobulins [41,42]. As of yet, it has not been established whether N-glycans on the Notch1 receptor are core fucosylated, though it has been noted that aberrant activity of both Fut8 and Notch is regularly observed in cancer [43].

Lectins have become a powerful experimental tool to determine the N-glycan profile of a glycoprotein, as they are highly specific carbohydrate-binding proteins with no catalytic activity [44]. They can bind mono- or oligosaccharides and can recognise and distinguish between distinct branching and linkage patterns [45]. Several lectin binding assays have been developed and optimised which exploit the high level of specificity seen in lectin-oligosaccharide binding to determine the glycosylation profile of a given glycoprotein. Unlike mass spectrometry and HPLC, these assays do not require the chemical or enzymatic removal of carbohydrates from proteins [46].

The aim of this study was to characterise the profile of N-glycosylation of the Notch1 receptor and explore the impact of these N-glycans on ligand induced Notch1 signalling, receptor trafficking and Notch-mediated myogenic differentiation of S100β vascular stem cells *in vitro*.

Results

Jagged-1 (Jag-1) activation of the Notch1 receptor promotes myogenic differentiation

Mouse aortic vascular stem cells (mVSCs) and C3H 10T1/2 embryonic fibroblasts were both positive for S100β and Sca1 expression, while negative for SMC markers, Cnn1 and Myh11 [Fig S1(a), Figure 1(a)]. S100β mVSCs exhibited increased telomere length and telomerase activity (indicators of stemness), when compared to aortic tissue and cultured SMCs [Fig S1(b), (c)], and were capable of lineage specification following treatment with adipogenic and osteogenic differentiation media, respectively [Fig S1(d), (e)].

Immobilised recombinant Notch ligand, Jagged-1 increased the number of SMC-like/myogenic Cnn1 positive cells (40.5 ± 5%, $p<0.05$ n=6) in S100β mVSCs cultures, when compared to the Fc-IgG control (0.1 ± 0.4%) [Figure 1(b), (c)] concomitant with a significant increase in the expression of Notch target gene, *Hey1* and the late SMC differentiation marker gene, *Myh11*, an effect attenuated following pre-treatment of the cells with the γ-secretase inhibitor, DAPT [Figure 1(d),(e)].

Notch1 receptor depletion following siRNA knockdown at a transfection efficiency of > 80% [Fig S2(a)] reduced *Notch1* mRNA [Fig S2(b)] and Notch1 protein [Fig S2(c)] levels and significantly attenuated Jagged-1 induced *Hey1* [Figure 1(f)] and *Myh11* [Figure 1(g)] mRNA levels in S100β mVSCs, when compared to the scrambled control.

Chemical inhibition of N-glycosylation impairs Jagged-1 induced Notch signalling

TNC and DMJ are both chemical inhibitors of N-glycosylation [32,33]. N-glycan analysis was assessed in whole cell lysates and immunoprecipitated Notch1 samples from control, TNC and DMJ treated cells respectively, by measuring lectin binding using a series of commercial lectins (Table I). The binding characteristics of each lectin have previously been described [46].

133 The optimal concentrations of TNC (0.3 - 0.7µg/mL) and DMJ (2.0 - 4.0µg/mL) required to
134 reduce lectin binding in whole cell lysates was first evaluated before their effect on the N-glycan
135 profile of the immunoprecipitated Notch1 receptor [Fig S2(d)] following ectopic expression [Fig
136 S3(a)] was assessed. There was a dose-dependent decrease in absorbance from whole cell lysates,
137 indicating a reduction in lectin binding, following treatment of S100β mVSCs with TNC when
138 compared to the non-treated control cells [Figure 2(a)]. Maximum inhibition was observed at
139 0.5µg/mL (in the cases of WGA and E-PHA). Similarly, DMJ treatment caused a significant
140 reduction in binding across all lectins compared to the non-treated control with maximal
141 inhibition observed at 4.0µg/mL [Figure 2(c)]. A similar dose-dependent decrease in lectin
142 binding was observed in whole lysates following treatment of C3H10T1/2 cells with TNC [Fig
143 S4(a)] and DMJ [Fig S4(b)], but only in WGA and E-PHA. No significant change in binding was
144 detected at any DMJ concentration with ConA or LCA [Fig 4S (b)].

145 Lectin binding was significantly reduced in the immunoprecipitated Notch1 preparation from
146 S100β mVSCs treated with both TNC [Figure 2(b)] and DMJ [Figure 2(d)] across all lectins other
147 than WGA. Inhibition by DMJ was as pronounced as that of TNC. The increase in *Hey1* and
148 *Myh11* mRNA levels by Jagged-1 was significantly reduced in TNC [Figure 2(e),(f)] and DMJ
149 [Figure 2(g),(h)] treated S100β mVSCs, when compared to untreated control cells. In a similar
150 manner, recombinant Jagged-1 significantly increased *Hey1* and *Myh11* expression in C3H10T1/2
151 cells when compared to IgG-Fc, an effect that was significantly reduced in TNC treated [Fig
152 S4(d), (e)] and DMJ treated cells [Fig S4(f), (g)]. Interestingly, TNC treatment also led to a
153 significant decrease in *Hey1* expression in the Fc-treated control sample [Fig S4(d)]. This
154 decrease in *Hey1* expression following TNC and DMJ treatment was not due to changes in the
155 expression of the Notch1 receptor as there was no significant change in either *Notch1* transcript
156 levels or Notch1 protein expression following TNC or DMJ treatment, compared to the non-
157 treated control [Fig S3(c), (d)].

158 While ectopic expression of the Notch1 NICD [Fig S3(a), (b)] significantly increased *Hey1* and
159 *Myh11* mRNA levels in S100β mVSCs [Figure 3(a), (c)], there was no reduction in *Hey1* mRNA
160 following treartment of cells with TNC or DMJ, when compared to the vector control [Figure
161 3(a), (c)]. In contrast, *Myh11* mRNA levels were significantly reduced by the same treatment
162 [Figure 3(b), (d)]. These data suggest that Notch signalling elements after cleavage of the NICD
163 and the activation of *Hey1* gene are unaffected by TNC or DMJ, but components of the myogenic
164 differentiation pathway are altered by these treatments. Overall, inhibition of global
165 glycosyltransferase activity with TNC and DMJ reduced the level lectin binding of the Notch1
166 receptor, an effect concomitant with a significant reduction in ligand-induced Notch target gene
167 expression and myogenic differentiation of S100β mVSCs . This affect appears to be primarily at
168 the level of the Notch1 receptor for activation of Notch target gene expression, as NICD induced
169 target gene expression was unaffected. However, Notch1 NICD induced myogenic differention is
170 susceptible to inhibition following global removal of N-Glycans.

171 **GnT-III and Fut8 depletion impairs Jagged-1 induced Notch signalling**

172 *Mgat3* and *Fut8* genes code for the glycosyltransferases GnT-III and Fut8, respectively [39,51]. To
173 deplete their levels, targeted siRNA knockdown was performed in S100β mVSCs [Fig S3(e), (f)]
174 and C3H10T1/2 cells [Fig S5(a), (b)], respectively, before the N-glycan profile of whole lysates
175 [Figure 4(a)] and immunoprecipitated Notch1 [Figure 4(b)] was assessed by lectin binding using
176 the ELLA assay. There was a significant reduction in lectin binding of whole lysates following
177 *Mgat3* knockdown for ConA and E-PHA lectins in both S100β mVSCs [Figure 4(a)] and
178 C3H10T1/2 cells [Fig S4(c)] compared to the scrambled control, while no significant reduction in

179 binding was detected with the LCA or WGA lectins. In the case of the *Fut8* knockdown, this led
180 to a significant decrease in LCA binding in both cell lines, while any changes in binding with the
181 other three lectins was statistically insignificant [Figure 4(a), Fig S4(c)]. In parallel cultures,
182 *Mgat3* knockdown in S100β mVSCs resulted in a significant reduction in lectin binding of
183 immunoprecipitated Notch1with both the ConA and E-PHA lectins compared to the scrambled
184 control, while no significant reduction in binding was detected with LCA or WGA lectins [Figure
185 4(b)]. Meanwhile, *Fut8* knockdown led to significant decreases in ConA and LCA binding, but
186 not for WGA or E-PHA lectins [Figure 4(b)].

187 The repercussions of *Mgat3* and *Fut8* knockdown on Jagged-1 induced Notch signalling and
188 myogenic differentiation revealed a significant reduction in Jagged-1 stimulated *Hey1* and *Myh11*
189 expression in S100β mVSCs and C3H10T1/2 cells following both *Mgat3* knockdown [Figure
190 4(c), (d), Fig S5(c), (d)] and *Fut8* knockdown, respectively [Figure 4(e), (f), Fig S5(e), (f)], when
191 compared to the scrambled controls. In contrast, Notch1 NICD induced Notch signalling and
192 myogenic differentiation of S100β mVSCs was unaffected by *Mgat3* [Figure 5(a), (b)] and *Fut8*
193 knockdown [Figure 5(c), (d)], when compared to the empty vector (EV) controls. Moreover, the
194 decrease in *Hey1* expression following *Fut8* knockdown in S100β mVSCs was not due to changes
195 in the expression of the Notch1 receptor as there was no significant change in either Notch1
196 protein expression [Figure 5(e, f)] or *Notch1* mRNA levels [Figure 5(g)] following knockdown,
197 compared to scrambled control. In contrast, while there was a slight albeit significant change in
198 the expression of Notch 1 protein levels following *Mgat3* knockdown [Figure 5(e), (f)] this was
199 not reflected in changes to *Notch1* mRNA levels [Figure 5(g)].

200 **Inhibition of N-glycosylation impairs Notch receptor trafficking and degradation.**

201 N-glycosylation has been shown to be an essential modification for correct protein trafficking
202 from the endoplasmic reticulum (ER) and Golgi apparatus (GA) to their site of action within the
203 cell [26,47]. Therefore, the possibility that inhibition of N-glycosylation by either chemical inhibitor
204 (TNC or DMJ) or knockdown of *Mgat3* and *Fut8* interferes with Notch1 protein trafficking and
205 localisation to the membrane was explored. Membrane fractionation of crude lysate from S100β
206 mVSCs revealed the presence of distinct protein band profiles between each fraction, confirmed
207 using pan-cadherin, a ubiquitously expressed membrane-bound protein [Figure 6(a)].
208 Fractionation revealed that the transmembrane Notch1 protein is exclusively present in the
209 membrane fraction and absent in the cytosolic fraction [Figure 6(a)]. Following treatment of the
210 cells with TNC or DMJ for 48 h, there was a significant reduction in the expression of Notch1 in
211 the membrane fraction [Figure 6(b), (d)]. Brefeldin A (BFA), as a potent inhibitor of protein
212 transport in the Golgi apparatus, served as a positive control. Since cellular Notch1 protein levels
213 remained unchanged following treatment with TNC and DMJ [Fig S3(c), (d)], it is unlikely that
214 TNC and DMJ treatment was causing endocytosis and degradation of the receptor [Figure 6(b)].
215 This observation was further supported by immunocytochemical analysis of Notch1 localisation
216 *in situ*. Golgin97 served as a control to visualise the subcellular location of the GA [Figure
217 7(a),(c)]. The ratio of both the fluorescence intensity and density significantly decreased
218 following treatment with TNC, DMJ or BFA [Figure 7(c)] wherein a significant decrease in the
219 ratio of membrane:perinuclear localisation of Notch1 was observed following treatment [Figure
220 7(a), (c)]. Lower ratios indicate a higher level of fluorescence in the perinuclear region compared
221 to that at the membrane. This analysis suggests an accumulation of Notch1 in the perinuclear
222 region of the cell in response to TNC and DMJ treatment, similar to BFA [Figure 7(a), (c)] and
223 supports a significant reduction of Notch1 protein trafficking following inhibition of N-
224 glycosylation.

225 In a similar manner, membrane fractionation was used to determine whether knockdown of
226 *Mgat3* and *Fut8* also reduced Notch1 localisation to the membrane. There was a significant
227 reduction in the expression of Notch1 in the membrane fraction following *Mgat3* knockdown,
228 compared to the scrambled control. In contrast, there was no significant change following *Fut8*
229 knockdown [Figure 6(c), (e)]. This analysis suggests that Notch1 trafficking from the GA to the
230 plasma membrane is inhibited by *Mgat3* knockdown. However, in parallel experiments,
231 immunocytochemical analysis of Notch1 localisation *in situ* following knockdown of *Mgat3* and
232 *Fut8* demonstrated that there was no significant change in the ratio of either the fluorescence
233 intensity or density following knockdown whereas both ratios decreased significantly following
234 treatment BFA [Figure 7(b), (d)]. Therefore, it is more likely that this reduction is due to the
235 decrease in total Notch1 protein in the cell following *Mgat3* knockdown [Figure 5(e)].

236 In summary, knockdown of the *GnT-III* and *Fut8* glycosyltransferases provided a more specific
237 insight into how two groups of N-glycans (bisected and core fucosylated) contributed to Notch
238 signalling and myogenic differentiation. Knockdown of the *Mgat3* transcript (which codes for the
239 GnT-III protein) led to a reduction in E-PHA binding, while *Fut8* knockdown resulted in a
240 decreased level of LCA binding. These findings provide evidence for the presence of both
241 complex bisecting and core fucosylated N-glycans on the Notch1 receptor. Moreover, knockdown
242 of *GnT-III* and *Fut8* glycosyltransferases demonstrated that both groups of N-glycans play a
243 major role in activation of both Notch target gene expression and myogenic marker expression
244 following Jagged-1 activation of mVSCs.

245 **Site-directed mutagenesis of six N-glycosylation impairs Jagged-1 induced Notch signalling**

246 Specific targeting of individual glycans to further define the function of both bisecting and core
247 fucosylated N-glycans was performed through site-directed mutagenesis of the six N-
248 glycosylation consensus sequences along the Notch1 ECD. Site-directed mutagenesis of plasmid-
249 encoded Notch1 was chosen, and the proportion of transfected cells was maximised in each
250 population through puromycin selection [Fig S6(a), (b)]. The optimum concentration of plasmid
251 DNA was assessed using a green fluorescent protein (GFP)-coding plasmid [Fig S6(b)]. Using
252 the *pCS2 Notch1 Full Length-6MT* plasmid, six single base substitutions were carried out
253 separately on the Notch1 gene to alter asparagine residues at amino acid positions 888, 959, 1179,
254 1241, 1489 and 1587 to isoleucine residues. Mutant plasmids were sequenced and aligned with
255 the wild- type plasmid sequence using Multalin to confirm that the correct single base substitution
256 had been incorporated in each case. In each case an essential adenine base was correctly
257 converted to a thymine base [Fig S7(a)]. Chromatograms were also generated to determine the
258 quality of both the sequencing read and the sample plasmid and confirmed high quality with
259 clearly defined peaks [Fig S7(b)].

260 Mutations at N888I, N1489I and N1587I all resulted in a significant decrease in ConA, LCA and
261 E-PHA binding compared to that observed in the wild-type cells but did not significantly alter
262 WGA binding. N959I led to a significant reduction only in ConA binding, while N1179I caused a
263 significant attenuation in only the binding of LCA [Figure 8(a)]. In parallel cultures, Jagged-1
264 significantly increased the expression of *Hey1* in control wild-type Notch1 transfected cells, an
265 effect that was significantly attenuated by mutations N888I, N1241I and N1587I of the Notch1
266 ECD [Figure 8(b)] concomitant with a significant reduction in Jagged-1 induced *Myh11*
267 expression [Figure 8(b)].

268 The changes in *Hey1* or *Myh1*1 expression were not attributed to a discrepancy in efficiency of
269 plasmid transfection across mutants as there was no significant difference between levels of

Notch1-coding plasmid DNA across all mutant plasmid samples compared to the wild-type control [Fig S8(a)]. However, a significant decrease in Notch1 protein levels was observed in cells transfected with mutants N1241I and N1587I, respectively, while no significant change was detected across all other mutants, compared to the wild-type control [Figure 8(d)]

These data indicate that all the mutations incorporated into the Notch1 gene, except N1241, had a measurable effect on receptor glycosylation. Lectin binding indicated the presence of a range of different N-glycan structures on the Notch1 ECD, including core fucosylated and bisecting N-glycans, and some additional structures that could not be identified with the limited range of lectins used. Mutation of asparagine residues at Notch1 N-glycosylation sites reduced *Hey1* expression (N888I, N1241I and N1587I) and *Myh11* expression (all mutations) following Jagged-1 stimulation. This was not due to altered plasmid transfection efficiency, but for some mutants (N1241I and N1587I), altered expression and/or degradation of Notch1 may be involved. It is likely that the N-glycans at the four other mutation sites may influence Notch1 processing and signalling, such as receptor cleavage or trafficking.

Discussion

Glycosylation is an essential regulator of many cellular processes and Notch signalling is no different [26]. In contrast to the well documented role of O-glycosylation, very little is known about the structure and function of Notch1 N-linked glycans. Here we report on bisecting and core fucosylated N-glycans decorating the extracellular domain (ECD) of the Notch1 receptor and their putative role in ligand-induced Notch signalling and myogenic differentiation of resident vascular stem cells *in vitro.* O-glycosylation is well established as influencing the folding, trafficking, activation, and cleavage of Notch1[47–50]. Although it has been shown that there are six highly conserved N-glycosylation sites on the Notch receptor [30], there is currently no data available to determine how many of these sites are glycosylated and what type of N-glycans reside on the receptor, other than data that suggests the Notch1 receptor contains complex bisecting N-glycans [51]. The Notch signalling pathway, and the Notch1 receptor in particular, plays an important role in lineage specification *in vitro* and vascular lesion formation *in vivo* [19,20]. Therefore, this study sought to characterise the profile of N-glycosylation of the Notch1 receptor and explore the impact of removing these N-glycans on Notch signalling and on Notch-mediated myogenic differentiation of S100β vascular stem cells.

The Notch signalling pathway drives myogenic specification of a range of stem cells, including S100β resident mVSCs[21,22,52]. Herein, immobilised recombinant Jagged-1 was used to activate the Notch receptor and stimulate the expression of both Notch target genes and myogenic genes in S100β mVSCs. Canonical Notch signalling operates via the NICD-RBP-Jκ complex which, along with other transcription factors, activates Notch target gene expression [2]. The NICD-RBP-Jκ complex is essential for maintaining SMC differentiation [53,54] through interaction with the serum response factor (SRF)-myocardin transcription activator complex [55]. However, several studies have described the ability of Notch target genes, such as *Hey1* and *Hey2*, to inhibit myocardin-induced SMC differentiation, although many of these studies differ in their description of the mechanism of inhibition, with some citing a direct interaction between Notch target genes and SRF, while others suggest that this occurs via an independent parallel pathway [56,57]. While it has been well documented that Notch target genes such as *Hey1* and *Hes1* contain RBP-Jκ binding domains at specific GTGGGAA consensus sequences within their promoter regions [2], bioinformatic analysis of the *Myh11* and *Cnn1* promoter regions suggests this consensus sequence is also present within their promoter [58]. Moreover, CBF1 (the human form of RBP-Jκ) interacts with SMAD2/3 in the TGF-β signalling pathway to promote transcription of SMC genes

independent of myocardin, such as *Cnn1* and *SM22α,* albeit this interaction was not observed with Notch1. While NICD induced Notch signalling in S100β mVSCs promotes Notch target gene and myogenic gene expression in S100β mVSCs, the Jagged-1 response was dependent on canonical Notch signalling as the γ-secretase inhibitor, DAPT effectively abrogated this response.

Mammalian cells express four different types of Notch receptor (Notch1 - 4) and each one can initiate downstream Notch signal transduction in target cells [2]. In agreement with previous studies, knockdown of *Notch1* mRNA in S100β mVSCs significantly attenuated Jagged-1-induced Notch target gene and myogenic gene expression confirming the pivotal role of Notch1 in lineage specification of these cells during lesion fromation [10,11]. Future studies that selectively delete the Notch1 receptor in resident S100β mVSCs using *S100β-CreERT2* transgenic mice crossed with Notch1 floxed mice before vascular injury will reveal the importance of this data *in vivo,* in addition with studies that explore the role of the other three Notch receptors in this process. In this context, loss of Notch 2 in SMCs leads to protein profile changes during lesion formation but does not alter overall lesion morphology or cell proliferation [59]. Nevertheless, the current findings highlight the potential of Notch1 as a therapeutic target for controlling the accumulation of SMC-like cells from mVSCs in arteriosclerotic lesion progression.

To date, evidence regarding the profile of N-linked glycans on the Notch1 receptor suggests that six consensus sites are present and highly conserved along the ECD, and that at least some of the N-glycans at these sites contain a bisecting structure [30,60]. In the current study, lectin binding analysis of the purified Notch1 receptor confirmed the presence of N-glycans, and of bisecting N-glycans, whilst also revealing the existence of oligosaccharides with a fucose residue bound to the core GlcNAc by an α-1,6 linkage (referred to as core fucosylation). Treatment with global N-glycosylation inhibitors tunicamycin (TNC) and 1-deoxymannojirimycin (DMJ) further supported these findings as each inhibitor promoted a reduction in binding of the E-PHA (specific for bisecting structures) and LCA (specific for core fucosylated structures) lectins to the purified Notch1 protein. However, many lectins have weak affinity for oligosaccharide structures other than their main binding target, including both E-PHA and LCA [61,62]. To further confirm the type of structures bound by these lectins, a siRNA knockdown was implemented to inhibit the expression of the key glycosyltransferases responsible for the formation of bisecting and core fucosylated N-glycans, namely GnT-III and Fut8, respectively.

Knockdown of the *Mgat3* and *Fut8* glycosyltransferase-coding genes had a significant effect on bisecting or core fucosylated N-glycans of Notch1, supporting the TNC and DMJ inhibition studies. *Mgat3* and *Fut8* knockdown also reduced the level of ligand mediated Notch signalling and myogenic differentiation in both mVSCs and C3H 10T1/2 cells. As downstream components of Notch signalling and myogenic differentiation pathways following ectopic expression of Notch1 NICD were not altered by *Mgat3* or *Fut8* knockdown, their effect appears to be primarily on the Notch1 receptor. Furthermore, as Notch1 transcript levels were not affected by either knockdown, but Notch1 protein expression was significantly reduced by *Mgat3* expression, these data suggests that bisecting N-glycans may have a role in preventing the degradation of the Notch1 receptor. The function of core fucosylated N-glycans is more difficult to decipher as reduction of their synthesis through *Fut8* knockdown had no effect on Notch1 protein expression or on receptor trafficking but caused a significant attenuation of Notch signalling and myogenic differentiation. There may be an alternative function for core fucosylated N-glycans on the Notch1 receptor, such as regulating cleavage events. Our finding that inhibition of GnT-III blocks Notch activation suggests that targeting GnT-III or blocking bisecting glycosylation sites on the Notch1 receptor may lead to new therapeutics targeting neointimal formation. Overall, the evaluation of GnT-III expression levels could also have clinical utility for stratifying patient cohorts that could benefit from therapies that target Notch1 signalling.

365 The impact of N-linked glycosylation on O-fucose glycosylation of Notch is not known. The N-
366 linked sites within Notch1 ECD are in close proximity to O-fucose modified sites. O-Fucose
367 glycosylation of Notch EGF repeats has been shown to create a code to either inhibit or activate
368 Notch ligand-dependent activation [65]. It will be important in the future to determine how the
369 bisecting glycan structures on the Notch1 receptor in mVSCs alter this O-fucose code. While the
370 importance of O-linked glycosylation in Notch receptor-ligand binding and receptor processing
371 and trafficking is well documented [27,29,66], little information is available on the role of N-glycans
372 in this context. Further investigation into how TNC and DMJ attenuated the Jagged-1 response
373 revealed that it was mediated by preventing Notch1 receptor trafficking out of the ER-Golgi
374 complex to the plasma membrane. A similar effect on Notch 3, where TNC treatment resulted in
375 accumulation of the receptor in the ER-Golgi complex, has been reported [67]. While this may be
376 due to changes in glycosylation of the numerous proteins involved in receptor trafficking,
377 multiple previous reports have demonstrated that inhibiting the N-glycosylation of developing
378 proteins can block their transport to the membrane [68,69]. Therefore, it is likely that some of the N-
379 glycans on the Notch1 ECD are required for correct trafficking of the protein to the plasma
380 membrane. Unlike TNC and DMJ treatment, knockdown of GnT-III and Fut8 did not affect
381 downstream elements of either Notch signalling or myogenic differentiation pathways, indicating
382 that bisecting and core fucosylated N-glycans exert their influence on the Jagged-1 response
383 either at, or before, the point of Notch receptor activation. Indeed, analysis of receptor trafficking
384 suggests that inhibition of the glycosyltransferase did not result in accumulation of Notch1 in the
385 ER-Golgi complex, as was seen with chemical inhibition of N-glycosylation. This suggests that
386 the inhibition of trafficking observed following TNC and DMJ treatment was either due to altered
387 glycosylation of transport proteins or removal of N-glycans on the Notch1 receptor which do not
388 contain bisecting or core fucosylated structures. A combination of receptor trafficking data and
389 measurement of Notch1 protein levels suggests that bisecting N-glycans prevent the accelerated
390 degradation of the Notch1 receptor. This supports previous studies showing Notch1 receptor
391 colocalization with lysosomal degradation proteins following *Mgat3* knockdown [51]. The role of
392 core fucosylated N-glycans may be more directly related to the activation of the Notch1 receptor
393 as knockdown of the *Fut8* glycosyltransferase inhibited Notch signalling and myogenic
394 differentiation but did not affect Notch1 expression, trafficking, degradation, or downstream
395 signalling.

396

397 Collectively, the data confirm a role for N-linked bisecting glycosylation in the ligand activation
398 of Notch1 in S100β mVSCs. However, as both chemical inhibition and knockdown of *Mgat3* and
399 F*ut8* could also alter the N-glycosylation of proteins other than the Notch1 receptor, it is possible
400 that these interventions could influence Notch downstream signalling capacity. Indeed, nicastrin,
401 for example, is part of the γ-secretase complex which cleaves the NICD from the Notch1
402 transmembrane domain (TMD) following receptor activation, and it contains bisecting N-glycans
403 which may be crucial for its role in the cleavage process [60,63]. Similarly, *Fut9* knockdown of core
404 fucosylated N-glycans impairs the proliferation of S100β neural stem cells via inhibition of
405 Musashi-1 (Msi-1), an RNA-binding protein and activator of the Notch signalling pathway, that
406 binds to *Numb* mRNA and inhibits its translation. *Fut9* knockdown is coupled with increased
407 Numb levels eventually resulting in the suppression of Notch signalling [64]. Therefore, the
408 reduction in Notch target gene and myogenic gene expression following *Mgat3* and *Fut8*
409 knockdown may have been due, at least in part, to removal of N-glycans (bisected and core
410 fucosylated) from other key proteins impacting on Notch signalling in these cells. For this reason,
411 it was important to further explore the mechanisms by which core fucosylated and/or bisecting N-
412 glycans were affecting the Notch signalling process following site-directed mutagenesis of key
413 sites on the Notch1 ECD.

414 Site-directed mutagenesis of the six N-glycosylation consensus sequences along the Notch1 ECD
415 further defined the function of both bisecting and core fucosylated N-glycans. While initial
416 analysis indicated that the amino acid site N1241 may not be glycosylated, additional information
417 indicates that it is more likely that the N-glycan at this site was not detected due to the limited
418 range of lectins used and the low binding affinity of some lectins *in vitro*[70]. This is further
419 emphasised by the fact that the N1179 mutation did not lead to a significant change in ConA
420 binding, but did significantly reduce the level of LCA binding, indicating that a core fucosylated
421 oligosaccharide may be present at this site which was not detected by ConA. Similarly, analysis
422 of the N959 mutant indicated that an N-linked oligosaccharide is present at this site but does not
423 contain structures required for binding to LCA, WGA or E-PHA. Meanwhile, the glycan at site
424 N1179 was found to contain a core fucosylated structure. Finally, it is noteworthy that N-glycans
425 at N888, N1489 and N1587 shared a similar lectin binding profile with significant reduction in
426 the level of binding with ConA, LCA and E-PHA with these mutants, suggesting that glycans at
427 those sites are both core fucosylated and have a bisecting structure. Therefore, it is possible that
428 they share similar structural characteristics and that the N-glycans at those sites may be both core
429 fucosylated and have a bisecting structure. However, this is unlikely as it has previously been
430 demonstrated that GnT-III modification of an oligosaccharide actively inhibits the addition of a
431 fucose by Fut8 [71]. This discrepancy may be explained by the alternative binding specificities of
432 certain lectins. E-PHA predominantly binds to N-glycans containing a bisecting structure but has
433 also been shown to have affinity for oligosaccharides with terminal galactose residue [62,72] .
434 Similarly, LCA has very high binding affinity for α1,6-fucosylated glycans, but can also bind the
435 mannose core of an N-glycan in the absence of 213 core fucosylation [61]. Further investigation will
436 be required to decipher which structures they possess as data from the ELLA suggests the
437 presence of either a core fucosylated N-glycan with a possible terminal galactose residue, or a
438 bisecting N-glycan. Data from previous studies [51] along with glycosyltransferase knockdown and
439 chemical inhibition experiments in this study, suggests that at least one of these three sites
440 contains an N-glycan with a bisecting structure, with the most likely candidate being N1587 as
441 mutation of this residue resulted in the greatest reduction in E-PHA binding. Future studies using
442 additional mutations on both the essential asparagine residue and on other proximal non-essential
443 residues could reveal the impact of the amino acid alteration on protein expression, function, and
444 stability. Many studies which involve the mutation of N-glycosylation sites on a glycoprotein also
445 use simultaneous multi-site mutation to investigate whether the combined impact of losing two or
446 more N-glycans differs from the effect observed following loss of a single N-glycan [69,73,74]. This
447 is a strategy that could reveal crucial information about the synergistic roles of N-glycans on the
448 Notch1 ECD.

449 Regarding the mutations at sites N888, N1241 and N1587, their effect specifically prevents
450 canonical Notch signalling. Indeed, lectin binding data suggests that the N-glycan at N888
451 possessed either a bisecting or core fucosylated structure and in view of the evidence from
452 glycosyltransferase knockdown experiments, it is likely that its absence does not lead to
453 accumulation of Notch1 in the ER-Golgi complex. Furthermore, since the mutation at this site did
454 not result in any change to Notch1 protein levels in the cell, i.e., did not accelerate Notch1
455 degradation, this suggests that it is most likely a core fucosylated N-glycan (possibly with a
456 terminal galactose residue), rather than a bisecting N-glycan. Taken together, these data suggest
457 that the N-glycan at N888 has a direct influence on Notch1 signal activation at the membrane.
458 This may occur through regulation of processes such as receptor folding or cleavage, mechanisms
459 which are regularly affected by loss of an individual N-glycan on other membrane-bound proteins
460 [75–77]. The N1241I mutation resulted in a dramatic decrease in Notch1 protein levels in the cell,
461 implying that the Notch1 receptor was rapidly degraded, and as a result, Notch target gene
462 expression was inhibited. ELLA data suggested that there may have been no N-glycan present at

463 N1241 but evidence from this mutation experiment is a strong indication that an N-glycan does
464 indeed reside at this site but does not contain bisecting or core fucosylated structures. Removal of
465 the N-glycan at N1587 also reduced Notch1 protein levels, most likely through receptor
466 degradation. Combined with lectin binding data and evidence from the knockdown studies, the
467 cumulative data suggests that the oligosaccharide which resides at this site contains a complex
468 bisecting structure.

469 Notably, all six mutations resulted in a reduction of the myogenic differentiation of stem cells in
470 response to Jagged-1 stimulation. This further supports lectin binding data by confirming that N-
471 glycans reside at each of the six consensus sites and reinforces data from chemical inhibition and
472 glycosyltransferase knockdown experiments by demonstrating that all these glycans are involved
473 in the process of Notch-mediated myogenic differentiation. However, only the mutations at sites
474 N888, N1241 and N1587 significantly attenuated the expression of the Notch target gene *Hey1*,
475 suggesting that the other three mutations at sites N959, N1179 and N1489 have an indirect effect
476 on myogenic differentiation which is independent of canonical Notch signalling. In addition,
477 none of these three mutations led to significant changes in Notch1 receptor protein levels in the
478 cell. Their effect on myogenic differentiation may be related to non-canonical Notch signalling
479 pathways, such as the Wnt/β-catenin pathway[78,79]. The Notch1 receptor has been shown to
480 interact with activated β-catenin at the membrane [80]. While this interaction occurs at the
481 intracellular C- terminal of the Notch1 receptor and it is unlikely that any direct interaction takes
482 place between these glycans and β-catenin, it is possible that their absence leads to altered
483 processing/folding of the receptor which results in dysregulation of Wnt signalling and myogenic
484 differentiation (Table II).

485 Some limitations in this study include the narrow range of available lectins which are specific for
486 N-linked oligosaccharides. Most commercially available lectins exhibit their highest affinity for a
487 particular monosaccharide in a specific branching/linkage format. However, many of these
488 structures can be found in both O-linked and N-linked glycans, such as Erythrina critagalli lectin
489 (ECL) that bind strongly to the terminal galactose of an N-acetyllactosamine-containing N-
490 glycan, but will also bind to a terminal β1,4-galactose in O-glycans [81]. In addition, while
491 mutation of specific asparagine residues is a highly specific method, a single change in nucleotide
492 or amino acid sequence can have a dramatic effect on the expression, processing and/or function
493 of the target protein[74,82]. In this study, isoleucine was chosen as the substitute due the ease of
494 mutation (only a single base substitution required for each Asn site) and the non-reactive nature of
495 the side chain. However, the change in side-chain composition may alter the conformation of the
496 receptor or result in issues with steric hindrance [83]. While glutamine as a substitute is widely used
497 since its structure is the most similar to asparagine, the polar amide group of the glutamine
498 residue may lead to unwanted molecular reactions [84]. This can be circumvented by mutating the
499 Asn residue to a number of different amino acids, mutating the serine/threonine residue in the
500 consensus sequence, or mutating a proximal amino acid which is not part of the consensus
501 sequence [85]. Finally, alternative chemical inhibitors such as swainsonine, which blocks α-
502 mannosidase-II activity, could provide greater insights into the role of N-glycans while
503 knockdown of additional glycosyltransferases such as GnT-IV and ST3Gal1 could be useful in
504 deciphering the exact structures of N-linked oligosaccharides on the Notch1 receptor [31,86].

505 In conclusion, activation of the Notch1 receptor by its ligand, Jagged-1, stimulates myogenic
506 differentiation of resident S100β mVSCs. Furthermore, N-glycosylation intervention strategies,
507 including chemical inhibition, siRNA knockdown of the GnT-III and Fut8 glycosyltransferases,
508 and site-directed mutagenesis of N-glycosylation sites, reveal that this signalling is heavily
509 regulated by N-glycans which reside at six consensus sequences along the Notch1 ECD. Several
510 key oligosaccharides at these sites were found to contain bisecting or core fucosylated structures.
511 Notch1 expression and trafficking analysis indicated that N-glycans at asparagine (N) 1241 and

1587 protect the receptor from accelerated degradation, while the oligosaccharide at N888 directly affects signal transduction. Conversely, N-linked glycans at the other three sites do not impact canonical Notch1 signalling but still play a role in Notch-mediated myogenic differentiation, possibly via a non-canonical Notch signalling pathway.

The putative role of bisecting and core fucosylated N-glycans in ligand induced activation of the Notch1 receptor may present as a novel therapeutic target for controlling Notch1 signalling and myogenic differentiation of S100β resident vascular stem cells during subclinical atherosclerosis where these cells have been reported to play a major role in early lesion development [10–12].

Materials and Methods

Materials

A full list of the materials is available in Supplementary Materials

Cell Culture

Cells were grown in tissue culture flasks (25-175 cm^2) or in 6-well plates in a humidified incubator and were visualised by a Nikon Eclipse TS100 phase contrast microscope. S100β mouse vascular stem cells (mVSCs) were isolated from the aortic arch of female C57BL/6J mice (used in accordance with EU legislation (Directive 2010/63/EU)) as previously described and grown in maintenance medium (MM1) containing DMEM supplemented with 2% chick embryo extract, 1% FBS, 0.02 µg/ml, bFGF basic protein, B-27 Supplement, N-2 supplement, 1% Penicillin-Streptomycin, 50 nM 2-Mercaptoethanol and 100 nM retinoic acid[10]. These stem cells exhibited a uniform neural-like morphology in low density culture adopting a dendritic-like tree shape and retaining their morphological characteristics at low density throughout repeated passage. Cells were fed with MM1 every 2-3 days and passaged every 3-4 days or when ~70% confluent. Cells were routinely grown in MM and dissociated with 0.5X TrypLE and expanded. Cells were used at passage numbers below p25. C3H/10T1/2 embryonic fibroblasts have been extensively characterised as multipotent mesenchymal cells [52]. Clone 8 - CCL-226 cells were grown in EMEM basal media supplemented with 10% heat inactivated FBS and 1% Penicillin Streptomycin. Cells were used at passage numbers below P20 and were always sub-cultured before confluency surpassed 70% to prevent post-confluence inhibition. Freezing media consisted of EMEM with 10% FBS, 1% Pen-Strep and 5% DMSO.

Adipogenesis Differentiation

Adipogenic differentiation of mVSCs was performed using StemPro® adipogenesis differentiation medium in accordance with the manufacturer's recommendations. Briefly, cells were seeded at a density of 1 x 10^4 cells/cm^2 in their maintenance medium and left for two days before being washed with PBS twice followed by feeding with StemPro® adipogenesis differentiation media for 14 days. Cells were harvested and adipogenic differentiation was evaluated by measuring the expression level of lipoprotein lipase (*Lpl*) and fatty acid binding protein 4 (*Fabp4*).

Osteogenesis Differentiation

560 Osteogenic differentiation of mVSCs was performed using the StemPro® osteogenic
561 differentiation medium in accordance with the manufacturer's recommendations. Briefly, cells
562 were seeded at a density of 1 x 10^4 cells/cm^2 in their maintenance medium and left for two days
563 before being washed with PBS twice followed by feeding with StemPro® osteogenic
564 differentiation media for 21 days. Cells were harvested and osteogenic differentiation was
565 evaluated by measuring the expression level of alkaline phosphatase (*Alpl*) and Sclerostin (*Sost)*.
566
567 *Telomerase Activity Assay*
568
569 Cell lysates were prepared using the RIPA buffer method and diluted to a protein concentration of
570 10-750 ng/µL before telomerase activity was measured using a TRAPeze® XL Telomerase
571 Detection Kit. Briefly, PCR was carried out using fluorescein- labelled primers to amplify
572 telomeric repeats in the sample DNA. Higher telomerase activity meant that there were more
573 telomeric repeats to be amplified by the Taq polymerase, resulting in a more fluorescent product.
574 The PCR products were analysed in a Tecan Safire II fluorescent plate reader. Telomerase activity
575 was calculated by comparing the level of fluorescence detected in each sample to a standard curve
576 generated from a set of telomeric repeat standards. The telomerase activity of a sample was given
577 in TPG units.
578
579 *Plasmid Amplification and Purification*
580
581 *Transformation:* LB Agar (20g/L LB, 12g/L Agar) was made up in dH_2O and autoclaved to
582 sterilise. After cooling to 55ºC, appropriate antibiotics were added (ampicillin at 100µg/mL or
583 kanamycin at 50µg/mL). The agar was poured into sterile petri dishes, allowed to harden, and
584 stored at 4ºC. A sample (100ng) of plasmid DNA was mixed with 50µL of competent JM109
585 bacterial cells in a sterile microfuge tube. Tube was placed on ice for 30 mins. Cells were then
586 heat-shocked at 42ºC for 45 secs to allow plasmid DNA to cross the cell membrane. Tube was
587 placed back on ice for 2 mins. 500µL of SOC medium (20% tryptone, 5% yeast extract, 0.5%
588 NaCl, 1% 0.25M KCl, 2% 1M glucose) was added to the tube which was then incubated at 37ºC
589 for 45 mins. The contents of the tube were transferred to a LB Agar plate with appropriate
590 antibiotics. Plates were incubated overnight at 37ºC. A single colony was picked from the
591 transformation plate and inoculated in 5mL of LB broth (20g/L LB) with appropriate antibiotics.
592 This culture was incubated at 37ºC in a shaking incubator for 6-8 hours. 1.2mL of this culture was
593 then transferred to a sterile conical culture flask containing 250mL of LB broth with appropriate
594 antibiotic. Flask was incubated at 37ºC overnight in a shaking incubator. 50mL was removed
595 from the flask for plasmid purification. The rest was used to make stocks by supplementing with
596 50% glycerol and storing at -80ºC.
597
598 *Plasmid DNA Purification:* Plasmid DNA was purified from transformed bacterial cells using the
599 Invitrogen PureLink™ HiPure Plasmid Filter Midiprep Kit according to the manufacturer's
600 guidelines. A Nanodrop® ND-1000 Spectrophotometer was used to quantitate the DNA
601 concentration before DNA samples were interrogated by agarose gel electrophoresis and
602 visualised with the SynGene G-Box.
603
604 *RNA Extraction*
605
606 RNA was extracted from cells using the Promega Reliaprep™ RNA Miniprep System according
607 to the provided instructions. A Nanodrop® ND-1000 Spectrophotometer was used to quantitate
608 the RNA concentration before RNA samples were analysed by *Quantitative Reverse-*
609 *Transcription Polymerase Chain Reaction (qRT-PCR)*

610
611 *Quantitative Reverse-Transcription Polymerase Chain Reaction (qRT-PCR)*
612
613 Quantitative RT-PCR was performed using the Rotor Gene Q from Corbett Research, as
614 previously described [10]. A ubiquitously expressed reference gene, hypoxanthine guanine
615 phosphoribosyltransferase (*Hprt)* was used as a control. Two different kits were used for this
616 method depending on the primer set: Rotor-Gene SYBR® Green RT-PCR Kit (Qiagen, 204174)
617 and SensiFAST™ SYBR® No-ROX One-Step Kit (BioLine, BIO-72001). Samples were run in
618 triplicate for each primer set.
619
620 *Immunocytochemistry*
621
622 Immunocytochemical analysis of protein expression in cells was performed, as described
623 previously[10]. Fixed cells on coverslips were stained for expression of the intermediate myogenic
624 differentiation marker Calponin1 (Cnn1) and the calcium binding protein, S100β by incubating
625 overnight at 4ºC with antibody diluted to an appropriate concentration with 1% BSA in PBS.
626 Cells were washed x 3 and incubated at room temperature for 1 hr with the secondary antibody
627 (diluted with 1% BSA in PBS), protected from light. Nuclear staining was performed with DAPI
628 which was diluted to 1µg/mL. Coverslips were mounted before cell nuclei and antibody staining
629 was visualised and imaged using the Olympus DP-50 fluorescent microscope. The number of
630 positive cells was counted for each image and divided by the total number of cells in that image to
631 give a ratio, and subsequently a percentage, of antigen-positive cells.
632
633 *Transient Transfections*
634
635 Transfection of both plasmid DNA and single strand siRNA duplexes into cells was performed
636 using the Mirus Bio TransIT-X2® dynamic delivery system, according to the manufacturer's
637 guidelines after optimization. Cells were grown to ~ 80% confluency in the maintenance medium
638 before transfection. The transfection mix was made up in a sterile microfuge tube according to kit
639 protocol and incubated at room temperature for 30 minutes to allow transfection complexes to
640 form. This mixture was then added dropwise to the cell culture. Cells were incubated at 37ºC for
641 48 hours before harvesting. Transfection efficiency was assessed using a control GFP-plasmid or
642 TYE 563 DsiRNA (Mirius Bio), a fluorescently tagged siRNA. A non-transfected sample was
643 used as a negative control. Cells were incubated at 37ºC for 48 h before being fixed with 3.7%
644 formaldehyde. Nuclei were stained with DAPI, and coverslips were mounted onto slides before
645 being imaged using a Olympus DP-50 fluorescent microscope. The number of cells containing
646 GFP, or dye were counted and graphed as a percentage of the total number of cells. A transfection
647 efficiency of 99.6% was achieved in the dye-transfected sample, compared to 0% in the non-
648 transfected sample.
649
650 *Genomic DNA Extraction*
651
652 Genomic DNA was extracted from cells using the Bioline ISOLATE II Genomic DNA Kit
653 according to the manufacturer's instructions. Briefly, cells were washed and scraped into PBS
654 and pelleted by centrifugation at 1500 rpm for 5 minutes. The pellet was resuspended in lysis
655 buffer GL. Proteinase K and Lysis Buffer G3 were then added to the sample before incubation at
656 70ºC for 15 minutes. 99% ethanol was added to each sample to adjust DNA binding conditions.
657 Samples were loaded into columns containing a silica membrane and centrifuged at 11,000 x g for
658 1 minute. The flow-through was discarded and columns were washed twice in wash buffer.
659 Elution buffer was then added to each column. Samples were incubated at room temperature for 1

660 minute before centrifugation at 11,000 x g for 1 minute. The flow-through contained the purified
661 DNA.
662
663 *Protein Isolation and Quantitation*
664
665 Cells at >80% confluency were scraped into culture media and pelleted by centrifugation. The
666 supernatant was discarded, cells were resuspended in an appropriate volume of RIPA buffer and
667 incubated on ice for 30 minutes to induce cell lysis. The lysate was then clarified by
668 centrifugation at 8,000 x g for 20 minutes at 4ºC. The supernatant containing cellular proteins was
669 retained while the cell debris pellet was discarded. The Pierce™ BCA Protein Assay Kit was used
670 to quantitate the concentration of protein in the clarified cell lysate.
671
672 *Membrane Fractionation and Protein Isolation*
673
674 Isolation of proteins from the cell membrane was carried out using the Mem-PER Plus Membrane
675 Protein Extraction Kit according to the manufacturer's instructions. Cells were harvested and the
676 Mem-PER™ Plus Membrane Protein Extraction Kit was used to perform membrane fractionation
677 on the crude lysate according to the manufacturer's instructions. Protein concentration in both the
678 cytoplasmic fraction and membrane fraction was quantified by BCA Assay. Both samples were
679 run on an SDS-PAGE precast protein gel and subsequently transferred to a nitrocellulose
680 membrane. Staining with Ponceau S confirmed the difference in the presence of protein band
681 profiles between the two samples. Immunoblotting was then carried out with an anti-Notch1
682 antibody and chemiluminescent staining was used to visualise bands.
683
684 *Effect of TNC and DMJ on Membrane Localisation of Notch1*
685
686 Cells were treated in the absence or presence of TNC (0.5µg/mL), DMJ (4µg/mL), 1 x Brefeldin
687 A (BFA) at 37ºC for 48 h before being harvested. Membrane fractions were isolated using the
688 Mem-PER™ Plus Membrane Protein Extraction Kit, according to the manufacturer's instructions.
689 Protein concentration in the membrane fractions was measured by BCA Assay. Western blot was
690 then carried out and samples were immuno-probed using an anti-Notch1 antibody.
691 Chemiluminescent staining was used to visualise immunoblotting. Densitometry was carried out
692 using ImageJ to measure the intensity of Notch1 bands while β-actin, pan-cadherin and Ponceau S
693 staining was used as loading controls.
694
695 *Trafficking of Notch1 Receptor*
696
697 Cells were seeded at 5,000 cells/well onto sterile coverslips and treated with or without TNC
698 (0.5µg/mL), DMJ (4µg/mL), 1 x BFA at 37ºC for 48 h before being fixed with 3.7%
699 formaldehyde. Immunocytochemistry was then carried out and cells were stained using an anti-
700 Notch1 antibody with an IgG control antibody used as a secondary control. A control sample was
701 also stained with an anti-Golgin-97 antibody to visualise the subcellular location of the golgi
702 apparatus (GA). Nuclei were stained with DAPI. Samples were imaged using a fluorescent
703 microscope. ImageJ was used to calculate the mean fluorescence intensity and the integrated
704 density of fluorescence at both the cell membrane and in the perinuclear region (adjacent to the
705 nucleus, i.e., where the GA is located). Samples were graphed as a ratio of the fluorescence at the
706 membrane to the fluorescence in the perinuclear region.
707
708
709 *Purification of Notch1 by Immunoprecipitation*

710
711 Protein lysates were prepared, and the protein concentration measured by BCA assay.
712 Immunoprecipitation was carried out using Protein A-conjugated magnetic beads and either an
713 anti-Notch1 rabbit monoclonal antibody, a rabbit IgG control antibody, or a mouse IgG control
714 antibody. Following incubation with the antibody, supernatants (containing unbound proteins)
715 were transferred to a fresh tube and appropriately stored. Bound protein was eluted off the beads
716 by either 1X Laemmli Buffer or a 0.1M Glycine buffer (pH 2.0). Samples eluted with the glycine
717 buffer were neutralised using a 1M Tris buffer (pH 9.0). Both eluted bound proteins and
718 previously stored unbound protein samples were then run on an SDS-PAGE precast protein gel,
719 transferred to a nitrocellulose membrane, immuno-probed using an anti-Notch1 antibody and
720 visualised by TMB staining of the HRP-conjugated secondary antibody.
721
722 *Ectopic Expression of Myc-tagged Notch1 and NICD*
723
724 The pCS2 Notch1 full length-6MT and pCS2 Notch1 ICv-6MT plasmids were purchased from
725 Addgene (LGC Standards, Teddington, UK) as bacterial stabs. Plasmid-containing bacteria were
726 transferred to a 5mL culture with selective antibiotic at 37ºC for 8 hrs. 1.2mL of this culture was
727 then transferred to a 250mL secondary culture with selective antibiotics which was incubated
728 overnight at 37ºC. Plasmid DNA was isolated from this culture using the Invitrogen PureLink™
729 HiPure Plasmid Filter Midiprep Kit. To verify plasmid length and quality, plasmid DNA was
730 digested with an appropriate restriction enzyme. This served to linearise the DNA before running
731 plasmid samples through gel electrophoresis on an agarose gel. Visualisation of this gel under UV
732 light confirmed that plasmids were the correct length and that the stocks contained no
733 contaminating DNA. To validate the ectopic expression of both proteins, cells were grown to
734 ~80% confluency in 3 wells of a 6-well plate and transfected with either the Notch1 full-length
735 plasmid, the NICD plasmid or an empty vector plasmid (pCDNA3.1) using the TransIT-X2
736 Dynamic Delivery System. Cells were incubated at 37ºC for 48 h in MM1 before being harvested.
737 Protein was isolated and quantified by BCA assay. Western blot was then carried out, with all
738 samples being immuno-probed using an anti-Myc-tag antibody to stain for either the myc-tagged
739 Notch1 or myc-tagged NICD, and an anti-β-actin antibody was used as the loading control.
740
741 *Western Blot*
742
743 Following protein isolation and quantitation, samples were prepared for SDS-PAGE using a
744 precast SDS 10% polyacrylamide gel to perform electrophoresis and the Pierce™ G2 Fast Blotter
745 for protein transfer, as previously described [53]. Ponceau S staining confirmed that the transfer had
746 been successful. Blocking buffer (5% dried milk in TBS with 0.1% Tween) was added to the
747 membrane and incubated at room temperature for 1-2 h on a rocker before the membrane was
748 washed in TBST (50mM Tris, 150mM NaCl, 1mM $MnCl_2$, 1mM $CaCl_2$, 1mM $MgCl_2$, 0.1%
749 Tween-20) and incubated with the primary antibody (diluted with 5% BSA in TBST) overnight
750 on a rocker at 4ºC. Primary antibody was removed, membrane washed 3 times (5 minutes each)
751 with TBST, before incubation with an HRP-conjugated secondary antibody (diluted with 5% BSA
752 in TBST) on a rocker for 1 hr at room temperature. Fresh TMB was added to the membrane
753 which was then incubated on a rocker at room temperature for approx. 10 mins before the blot
754 was imaged using BioRad GelDoc EZ Gel System. Alternatively, Pierce™ ECL Western Blotting
755 Substrate was added to the membrane which was then incubated on a rocker at room temperature
756 for 5 minutes. The blot was then imaged using Syngene G-Box.
757
758 *Enzyme-Linked Lectin Assay (ELLA)*
759

All samples were diluted to the same concentration with 50µL of treated sample or control sample added in triplicate to each well of a 96-well plate. The plate was incubated overnight at 4ºC with gentle shaking. Wells were emptied and blocking buffer (0.5% PVA in PBS) added to each well. The plate was incubated for 2 hrs at room temperature with gentle shaking before wells were washed with TBST (50mM Tris, 150mM NaCl, 1mM $MnCl_2$, 1mM $CaCl_2$, 1mM $MgCl_2$, 0.1% Tween-20). Biotinylated lectins (50µL, 5µg/mL) were added to each well and incubated at room temperature for 1 hr with gentle shaking before wells were emptied and washed again with TBST. HRP-conjugated anti-biotin antibody (50µL, 1:10,000) was then added to each well and incubated at room temperature for 1 hour with gentle shaking. Wells were washed with TBST before a TMB substrate solution (90µL) was added and incubated for 10 minutes at room temperature with gentle shaking. Stop solution (10% H_2SO_4) was added to each well before the absorbance was measured at 450 nm in a plate reader.

N-glycosylation Profile of Purified Notch1

Cells were grown to ~80% confluency in 3 wells per 6-well plate. One well was not transfected while the TransIT-X2 Dynamic Delivery System was used to transfect the other two wells with either the Notch1 full-length plasmid or an empty vector control plasmid. Cells were incubated at 37ºC for 48 h in maintenance media (MM1) before being harvested. Protein was isolated and quantified by BCA assay. IP was carried out to purify the ectopically expressed Notch1 using Protein G-conjugated magnetic beads and an anti-Myc-tag antibody. The non-transfected sample was immunoprecipitated with a mouse IgG control antibody. Bound proteins were eluted off the magnetic beads using a 0.1M Glycine buffer (pH 2.0) and a 1M Tris buffer (pH 9.0) was used to neutralise the purified protein fraction. BCA assay was carried out again to determine the concentration of protein in each sample post-IP. ELLA was then applied to detect the presence of N-glycans in all three samples. Control wells containing PBS rather than a protein sample were used to determine the baseline for non-specific absorbance, while the mouse IgG control sample acted as the baseline for non-specific lectin- or antibody-binding to the IP eluate. Both baseline values were subtracted from sample absorbance values to decipher the true level of specific lectin binding. TBST acted as the vehicle control for all lectins.

Site-directed mutagenesis

Mutation of N-glycosylation sites on a plasmid-encoded Notch1 receptor was achieved using the Agilent QuikChange Lightning Site Directed Mutagenesis Kit, according to the manufacturer's instructions. Briefly, primers were specific for a region of the Notch1 gene containing an N-glycosylation site and were designed to incorporate a single base substitution in copies of the plasmid DNA template. PCR tubes were placed in an Applied Biosystems® Veriti® Thermal Cycler. A DpnI restriction enzyme was added to each tube of PCR products to degrade any parental template DNA. Mutant plasmids were then transformed into ultracompetent XL10-Gold bacterial cells via heat-shock at 42ºC. After allowing the cells to recover for 1 hour in NZY^+ broth at 37ºC, each transformation reaction was spread on an LB agar plate with Ampicillin (50µg/mL) and incubated at 37ºC overnight. Colonies were picked and inoculated in liquid LB. Transformed bacteria were grown and mutant plasmids were purified before sending them for sequencing with Source Biosciences to confirm that the correct single base substitution had been incorporated in each case.

Data Analysis and Statistics

809 The mean and standard deviation (or standard error margin) was calculated for all the technical
810 and biological replicates in each experiment and these values were used to plot the data. The
811 Kolmogorov-Smirnov normality test was used to analyse the spread of the data as it uses the most
812 stringent conditions. The outcome of the normality test (along with the number of samples and
813 parameters) dictated what type of significance test was carried out. In the case of data containing
814 only two samples, an unpaired t-test with Welch's correction was performed on normally
815 distributed data. For non-parametric (skewed) data, the Wilcoxon test was carried out to calculate
816 statistical significance. For data containing more than two samples, ANOVA testing was used to
817 perform multiple comparisons between all samples. This could be carried out using an ordinary
818 one-way (one parameter to compare) or two-way (two parameters to compare) ANOVA for
819 normalised data, or the Kruskal-Wallis test for non-parametric data. This would reveal the level of
820 statistical significance for both the data as a whole and between each sample.
821
822
823 **References**
824

825 1. MacGrogan, D., Münch, J., and de la Pompa, J.L. (2018). Notch and interacting signalling
826 pathways in cardiac development, disease, and regeneration. Nat Rev Cardiol *15*, 685–704.
827 10.1038/s41569-018-0100-2.

828 2. Bray, S.J. (2016). Notch signalling in context. Nat Rev Mol Cell Biol *17*, 722–735.
829 10.1038/nrm.2016.94.

830 3. Siebel, C., and Lendahl, U. (2017). Notch Signaling in Development, Tissue Homeostasis,
831 and Disease. Physiol Rev *97*, 1235–1294. 10.1152/physrev.00005.2017.

832 4. Katoh, M. (2017). Canonical and non-canonical WNT signaling in cancer stem cells and
833 their niches: Cellular heterogeneity, omics reprogramming, targeted therapy and tumor
834 plasticity (Review). Int J Oncol *51*, 1357–1369. 10.3892/ijo.2017.4129.

835 5. Chappell, J., Harman, J.L., Narasimhan, V.M., Yu, H., Foote, K., Simons, B.D., Bennett,
836 M.R., and Jørgensen, H.F. (2016). Extensive Proliferation of a Subset of Differentiated, yet
837 Plastic, Medial Vascular Smooth Muscle Cells Contributes to Neointimal Formation in
838 Mouse Injury and Atherosclerosis Models. Circ Res *119*, 1313–1323.
839 10.1161/CIRCRESAHA.116.309799.

840 6. Dobnikar, L., Taylor, A.L., Chappell, J., Oldach, P., Harman, J.L., Oerton, E., Dzierzak, E.,
841 Bennett, M.R., Spivakov, M., and Jørgensen, H.F. (2018). Disease-relevant transcriptional
842 signatures identified in individual smooth muscle cells from healthy mouse vessels. Nat
843 Commun *9*, 4567. 10.1038/s41467-018-06891-x.

844 7. Majesky, M.W., Horita, H., Ostriker, A., Lu, S., Regan, J.N., Bagchi, A., Dong, X.R.,
845 Poczobutt, J., Nemenoff, R.A., and Weiser-Evans, M.C.M. (2017). Differentiated Smooth
846 Muscle Cells Generate a Subpopulation of Resident Vascular Progenitor Cells in the
847 Adventitia Regulated by Klf4. Circ Res *120*, 296–311.
848 10.1161/CIRCRESAHA.116.309322.

849 8. Kramann, R., Goettsch, C., Wongboonsin, J., Iwata, H., Schneider, R.K., Kuppe, C.,
850 Kaesler, N., Chang-Panesso, M., Machado, F.G., Gratwohl, S., et al. (2016). Adventitial
851 MSC-like Cells Are Progenitors of Vascular Smooth Muscle Cells and Drive Vascular

852 Calcification in Chronic Kidney Disease. Cell Stem Cell *19*, 628–642.
853 10.1016/j.stem.2016.08.001.

854 9. Wan, M., Li, C., Zhen, G., Jiao, K., He, W., Jia, X., Wang, W., Shi, C., Xing, Q., Chen, Y.-
855 F., et al. (2012). Injury-activated transforming growth factor β controls mobilization of
856 mesenchymal stem cells for tissue remodeling. Stem Cells *30*, 2498–2511.
857 10.1002/stem.1208.

858 10. Di Luca, M., Fitzpatrick, E., Burtenshaw, D., Liu, W., Helt, J.-C., Hakimjavadi, R.,
859 Corcoran, E., Gusti, Y., Sheridan, D., Harman, S., et al. (2021). The calcium binding protein
860 S100β marks hedgehog-responsive resident vascular stem cells within vascular lesions. NPJ
861 Regen Med *6*, 10. 10.1038/s41536-021-00120-8.

862 11. Molony, C., King, D., Di Luca, M., Kitching, M., Olayinka, A., Hakimjavadi, R., Julius,
863 L.A.N., Fitzpatrick, E., Gusti, Y., Burtenshaw, D., et al. (2021). Disease-Relevant Single
864 Cell Photonic Signatures Identify S100β Stem Cells and their Myogenic Progeny in
865 Vascular Lesions. Stem Cell Reviews and Reports *17*, 1713–1740. 10.1007/s12015-021-
866 10125-x.

867 12. Yuan, F., Wang, D., Xu, K., Wang, J., Zhang, Z., Yang, L., Yang, G.-Y., and Li, S. (2017).
868 Contribution of Vascular Cells to Neointimal Formation. PLoS One *12*, e0168914.
869 10.1371/journal.pone.0168914.

870 13. Tang, Z., Wang, A., Yuan, F., Yan, Z., Liu, B., Chu, J.S., Helms, J.A., and Li, S. (2012).
871 Differentiation of multipotent vascular stem cells contributes to vascular diseases. Nat
872 Commun *3*, 875. 10.1038/ncomms1867.

873 14. Lyu, L., Li, Z., Wen, Z., He, Y., Wang, X., Jiang, L., Zhou, X., Huang, C., Wu, Y., Chen,
874 T., et al. (2023). Fate mapping RNA-sequencing reveal Malat1 regulates Sca1+ progenitor
875 cells to vascular smooth muscle cells transition in vascular remodeling. Cell Mol Life Sci
876 *80*, 118. 10.1007/s00018-023-04762-3.

877 15. Caolo, V., Schulten, H.M., Zhuang, Z.W., Murakami, M., Wagenaar, A., Verbruggen, S.,
878 Molin, D.G.M., and Post, M.J. (2011). Soluble Jagged-1 inhibits neointima formation by
879 attenuating Notch-Herp2 signaling. Arterioscler Thromb Vasc Biol *31*, 1059–1065.
880 10.1161/ATVBAHA.110.217935.

881 16. Lindner, V., Booth, C., Prudovsky, I., Small, D., Maciag, T., and Liaw, L. (2001). Members
882 of the Jagged/Notch gene families are expressed in injured arteries and regulate cell
883 phenotype via alterations in cell matrix and cell-cell interaction. Am J Pathol *159*, 875–883.
884 10.1016/S0002-9440(10)61763-4.

885 17. Li, Y., Takeshita, K., Liu, P.-Y., Satoh, M., Oyama, N., Mukai, Y., Chin, M.T., Krebs, L.,
886 Kotlikoff, M.I., Radtke, F., et al. (2009). Smooth muscle Notch1 mediates neointimal
887 formation after vascular injury. Circulation *119*, 2686–2692.
888 10.1161/CIRCULATIONAHA.108.790485.

889 18. Sakata, Y., Xiang, F., Chen, Z., Kiriyama, Y., Kamei, C.N., Simon, D.I., and Chin, M.T.
890 (2004). Transcription factor CHF1/Hey2 regulates neointimal formation in vivo and
891 vascular smooth muscle proliferation and migration in vitro. Arterioscler Thromb Vasc Biol
892 *24*, 2069–2074. 10.1161/01.ATV.0000143936.77094.a4.

893 19.Redmond, E.M., Liu, W., Hamm, K., Hatch, E., Cahill, P.A., and Morrow, D. (2014).
894 Perivascular delivery of Notch 1 siRNA inhibits injury-induced arterial remodeling. PLoS
895 ONE *9*. 10.1371/journal.pone.0084122.

896 20.Chen, Q., Yang, F., Guo, M., Wen, G., Zhang, C., Luong, L.A., Zhu, J., Xiao, Q., and
897 Zhang, L. (2015). miRNA-34a reduces neointima formation through inhibiting smooth
898 muscle cell proliferation and migration. J Mol Cell Cardiol *89*, 75–86.
899 10.1016/j.yjmcc.2015.10.017.

900 21.Kurpinski, K., Lam, H., Chu, J., Wang, A., Kim, A., Tsay, E., Agrawal, S., Schaffer, D.V.,
901 and Li, S. (2010). Transforming growth factor-beta and notch signaling mediate stem cell
902 differentiation into smooth muscle cells. Stem Cells *28*, 734–742. 10.1002/stem.319.

903 22.Doi, H., Iso, T., Sato, H., Yamazaki, M., Matsui, H., Tanaka, T., Manabe, I., Arai, M.,
904 Nagai, R., and Kurabayashi, M. (2006). Jagged1-selective notch signaling induces smooth
905 muscle differentiation via a RBP-Jkappa-dependent pathway. J Biol Chem *281*, 28555–
906 28564. 10.1074/jbc.M602749200.

907 23.High, F.A., Zhang, M., Proweller, A., Tu, L., Parmacek, M.S., Pear, W.S., and Epstein, J.A.
908 (2007). An essential role for Notch in neural crest during cardiovascular development and
909 smooth muscle differentiation. J Clin Invest *117*, 353–363. 10.1172/JCI30070.

910 24.Kopan, R., and Ilagan, M.X.G. (2009). The canonical Notch signaling pathway: unfolding
911 the activation mechanism. Cell *137*, 216–233. 10.1016/j.cell.2009.03.045.

912 25.Fortini, M.E. (2009). Notch signaling: the core pathway and its posttranslational regulation.
913 Dev Cell *16*, 633–647. 10.1016/j.devcel.2009.03.010.

914 26.Pandey, A., Niknejad, N., and Jafar-Nejad, H. (2021). Multifaceted regulation of Notch
915 signaling by glycosylation. Glycobiology *31*, 8–28. 10.1093/glycob/cwaa049.

916 27.Moloney, D.J., Shair, L.H., Lu, F.M., Xia, J., Locke, R., Matta, K.L., and Haltiwanger, R.S.
917 (2000). Mammalian Notch1 is modified with two unusual forms of O-linked glycosylation
918 found on epidermal growth factor-like modules. J Biol Chem *275*, 9604–9611.
919 10.1074/jbc.275.13.9604.

920 28.Acar, M., Jafar-Nejad, H., Takeuchi, H., Rajan, A., Ibrani, D., Rana, N.A., Pan, H.,
921 Haltiwanger, R.S., and Bellen, H.J. (2008). Rumi is a CAP10 domain glycosyltransferase
922 that modifies Notch and is required for Notch signaling. Cell *132*, 247–258.
923 10.1016/j.cell.2007.12.016.

924 29.Shao, L., Moloney, D.J., and Haltiwanger, R. (2003). Fringe modifies O-fucose on mouse
925 Notch1 at epidermal growth factor-like repeats within the ligand-binding site and the
926 Abruptex region. J Biol Chem *278*, 7775–7782. 10.1074/jbc.M212221200.

927 30. Takeuchi, H., and Haltiwanger, R.S. (2014). Significance of glycosylation in Notch
928 signaling. Biochem Biophys Res Commun *453*, 235–242. 10.1016/j.bbrc.2014.05.115.

929 31.Stanley, P. (2016). What Have We Learned from Glycosyltransferase Knockouts in Mice? J
930 Mol Biol *428*, 3166–3182. 10.1016/j.jmb.2016.03.025.

931 32.Heifetz, A., Keenan, R.W., and Elbein, A.D. (1979). Mechanism of action of tunicamycin
932 on the UDP-GlcNAc:dolichyl-phosphate Glc-NAc-1-phosphate transferase. Biochemistry
933 *18*, 2186–2192. 10.1021/bi00578a008.

934 33.Elbein, A.D. (1987). Inhibitors of the biosynthesis and processing of N-linked
935 oligosaccharide chains. Annu Rev Biochem *56*, 497–534.
936 10.1146/annurev.bi.56.070187.002433.

937 34.Rademacher, T.W., Parekh, R.B., and Dwek, R.A. (1988). Glycobiology. Annual Review of
938 Biochemistry *57*, 785–838. 10.1146/annurev.bi.57.070188.004033.

939 35.Narasimhan, S. (1982). Control of glycoprotein synthesis. UDP-GlcNAc:glycopeptide beta
940 4-N-acetylglucosaminyltransferase III, an enzyme in hen oviduct which adds GlcNAc in
941 beta 1-4 linkage to the beta-linked mannose of the trimannosyl core of N-glycosyl
942 oligosaccharides. J Biol Chem *257*, 10235–10242.

943 36.Gu, J., Nishikawa, A., Tsuruoka, N., Ohno, M., Yamaguchi, N., Kangawa, K., and
944 Taniguchi, N. (1993). Purification and characterization of UDP-N-acetylglucosamine:
945 alpha-6-D-mannoside beta 1-6N-acetylglucosaminyltransferase (N-
946 acetylglucosaminyltransferase V) from a human lung cancer cell line. J Biochem *113*, 614–
947 619. 10.1093/oxfordjournals.jbchem.a124091.

948 37.Longmore, G.D., and Schachter, H. (1982). Product-identification and substrate-specificity
949 studies of the GDP-L-fucose:2-acetamido-2-deoxy-beta-D-glucoside (FUC goes to Asn-
950 linked GlcNAc) 6-alpha-L-fucosyltransferase in a Golgi-rich fraction from porcine liver.
951 Carbohydr Res *100*, 365–392. 10.1016/s0008-6215(00)81049-6.

952 38.Song, Y., Aglipay, J.A., Bernstein, J.D., Goswami, S., and Stanley, P. (2010). The bisecting
953 GlcNAc on N-glycans inhibits growth factor signaling and retards mammary tumor
954 progression. Cancer Res *70*, 3361–3371. 10.1158/0008-5472.CAN-09-2719.

955 39.Staudacher, E., Altmann, F., Wilson, I.B., and März, L. (1999). Fucose in N-glycans: from
956 plant to man. Biochim Biophys Acta *1473*, 216–236. 10.1016/s0304-4165(99)00181-6.

957 40.Wilson, J.R., Williams, D., and Schachter, H. (1976). The control of glycoprotein synthesis:
958 N-acetylglucosamine linkage to a mannose residue as a signal for the attachment of L-
959 fucose to the asparagine-linked N-acetylglucosamine residue of glycopeptide from alpha1-
960 acid glycoprotein. Biochem Biophys Res Commun *72*, 909–916. 10.1016/s0006-
961 291x(76)80218-5.

962 41.Okazaki, A., Shoji-Hosaka, E., Nakamura, K., Wakitani, M., Uchida, K., Kakita, S.,
963 Tsumoto, K., Kumagai, I., and Shitara, K. (2004). Fucose depletion from human IgG1
964 oligosaccharide enhances binding enthalpy and association rate between IgG1 and
965 FcgammaRIIIa. J Mol Biol *336*, 1239–1249. 10.1016/j.jmb.2004.01.007.

966 42.Osumi, D., Takahashi, M., Miyoshi, E., Yokoe, S., Lee, S.H., Noda, K., Nakamori, S., Gu,
967 J., Ikeda, Y., Kuroki, Y., et al. (2009). Core fucosylation of E-cadherin enhances cell-cell
968 adhesion in human colon carcinoma WiDr cells. Cancer Sci *100*, 888–895. 10.1111/j.1349-
969 7006.2009.01125.x.

970 43. Pakkiriswami, S., Couto, A., Nagarajan, U., and Georgiou, M. (2016). Glycosylated Notch
971 and Cancer. Front Oncol *6*, 37. 10.3389/fonc.2016.00037.

972 44. Lis, H., and Sharon, N. (1998). Lectins: Carbohydrate-Specific Proteins That Mediate
973 Cellular Recognition. Chem Rev *98*, 637–674. 10.1021/cr940413g.

974 45. Ghazarian, H., Idoni, B., and Oppenheimer, S.B. (2011). A glycobiology review:
975 carbohydrates, lectins and implications in cancer therapeutics. Acta Histochem *113*, 236–
976 247. 10.1016/j.acthis.2010.02.004.

977 46. Thompson, R., Creavin, A., O'Connell, M., O'Connor, B., and Clarke, P. (2011).
978 Optimization of the enzyme-linked lectin assay for enhanced glycoprotein and
979 glycoconjugate analysis. Anal Biochem *413*, 114–122. 10.1016/j.ab.2011.02.013.

980 47. Fan, H., Meng, W., Kilian, C., Grams, S., and Reutter, W. (1997). Domain-specific N-
981 glycosylation of the membrane glycoprotein dipeptidylpeptidase IV (CD26) influences its
982 subcellular trafficking, biological stability, enzyme activity and protein folding. Eur J
983 Biochem *246*, 243–251. 10.1111/j.1432-1033.1997.00243.x.

984 48. Li, L.-B., Chen, N., Ramamoorthy, S., Chi, L., Cui, X.-N., Wang, L.C., and Reith, M.E.A.
985 (2004). The role of N-glycosylation in function and surface trafficking of the human
986 dopamine transporter. J Biol Chem *279*, 21012–21020. 10.1074/jbc.M311972200.

987 49. Matsumoto, K., Ayukawa, T., Ishio, A., Sasamura, T., Yamakawa, T., and Matsuno, K.
988 (2016). Dual Roles of O-Glucose Glycans Redundant with Monosaccharide O-Fucose on
989 Notch in Notch Trafficking. J Biol Chem *291*, 13743–13752. 10.1074/jbc.M115.710483.

990 50. Ogawa, M., Tashima, Y., Sakaguchi, Y., Takeuchi, H., and Okajima, T. (2020).
991 Contribution of extracellular O-GlcNAc to the stability of folded epidermal growth factor-
992 like domains and Notch1 trafficking. Biochem Biophys Res Commun *526*, 184–190.
993 10.1016/j.bbrc.2020.03.066.

994 51. Allam, H., Johnson, B.P., Zhang, M., Lu, Z., Cannon, M.J., and Abbott, K.L. (2017). The
995 glycosyltransferase GnT-III activates Notch signaling and drives stem cell expansion to
996 promote the growth and invasion of ovarian cancer. J Biol Chem *292*, 16351–16359.
997 10.1074/jbc.M117.783936.

998 52. Zhao, L., Li, G., Chan, K.-M., Wang, Y., and Tang, P.-F. (2009). Comparison of
999 multipotent differentiation potentials of murine primary bone marrow stromal cells and
1000 mesenchymal stem cell line C3H10T1/2. Calcif Tissue Int *84*, 56–64. 10.1007/s00223-008-
1001 9189-3.

1002 53. Morrow, D., Scheller, A., Birney, Y.A., Sweeney, C., Guha, S., Cummins, P.M., Murphy,
1003 R., Walls, D., Redmond, E.M., and Cahill, P.A. (2005). Notch-mediated CBF-1/RBP-Jκ-
1004 dependent regulation of human vascular smooth muscle cell phenotype in vitro. American
1005 Journal of Physiology - Cell Physiology *289*, C1188–C1196. 10.1152/ajpcell.00198.2005.

1006 54. Morrow, D., Guha, S., Sweeney, C., Birney, Y., Walshe, T., O'Brien, C., Walls, D.,
1007 Redmond, E.M., and Cahill, P.A. (2008). Notch and vascular smooth muscle cell
1008 phenotype. Circulation Research *103*, 1370–1382. 10.1161/CIRCRESAHA.108.187534.

1009 55.Noseda, M., Fu, Y., Niessen, K., Wong, F., Chang, L., McLean, G., and Karsan, A. (2006).
1010 Smooth Muscle alpha-actin is a direct target of Notch/CSL. Circ Res *98*, 1468–1470.
1011 10.1161/01.RES.0000229683.81357.26.

1012 56.Proweller, A., Pear, W.S., and Parmacek, M.S. (2005). Notch signaling represses
1013 myocardin-induced smooth muscle cell differentiation. J Biol Chem *280*, 8994–9004.
1014 10.1074/jbc.M413316200.

1015 57.Doi, H., Iso, T., Yamazaki, M., Akiyama, H., Kanai, H., Sato, H., Kawai-Kowase, K.,
1016 Tanaka, T., Maeno, T., Okamoto, E., et al. (2005). HERP1 inhibits myocardin-induced
1017 vascular smooth muscle cell differentiation by interfering with SRF binding to CArG box.
1018 Arterioscler Thromb Vasc Biol *25*, 2328–2334. 10.1161/01.ATV.0000185829.47163.32.

1019 58.Tang, Y., Urs, S., Boucher, J., Bernaiche, T., Venkatesh, D., Spicer, D.B., Vary, C.P.H.,
1020 and Liaw, L. (2010). Notch and transforming growth factor-beta (TGFbeta) signaling
1021 pathways cooperatively regulate vascular smooth muscle cell differentiation. J Biol Chem
1022 *285*, 17556–17563. 10.1074/jbc.M109.076414.

1023 59.Peterson, S.M., Turner, J.E., Harrington, A., Davis-Knowlton, J., Lindner, V., Gridley, T.,
1024 Vary, C.P.H., and Liaw, L. (2018). Notch2 and Proteomic Signatures in Mouse Neointimal
1025 Lesion Formation. Arterioscler Thromb Vasc Biol *38*, 1576–1593.
1026 10.1161/ATVBAHA.118.311092.

1027 60.Allam, H., Aoki, K., Benigno, B.B., McDonald, J.F., Mackintosh, S.G., Tiemeyer, M., and
1028 Abbott, K.L. (2015). Glycomic analysis of membrane glycoproteins with bisecting
1029 glycosylation from ovarian cancer tissues reveals novel structures and functions. J Proteome
1030 Res *14*, 434–446. 10.1021/pr501174p.

1031 61.Maupin, K.A., Liden, D., and Haab, B.B. (2012). The fine specificity of mannose-binding
1032 and galactose-binding lectins revealed using outlier motif analysis of glycan array data.
1033 Glycobiology *22*, 160–169. 10.1093/glycob/cwr128.

1034 62.Nagae, M., Soga, K., Morita-Matsumoto, K., Hanashima, S., Ikeda, A., Yamamoto, K., and
1035 Yamaguchi, Y. (2014). Phytohemagglutinin from Phaseolus vulgaris (PHA-E) displays a
1036 novel glycan recognition mode using a common legume lectin fold. Glycobiology *24*, 368–
1037 378. 10.1093/glycob/cwu004.

1038 63.Yu, G., Nishimura, M., Arawaka, S., Levitan, D., Zhang, L., Tandon, A., Song, Y.Q.,
1039 Rogaeva, E., Chen, F., Kawarai, T., et al. (2000). Nicastrin modulates presenilin-mediated
1040 notch/glp-1 signal transduction and betaAPP processing. Nature *407*, 48–54.
1041 10.1038/35024009.

1042 64.Yagi, H., Saito, T., Yanagisawa, M., Yu, R.K., and Kato, K. (2012). Lewis X-carrying N-
1043 glycans regulate the proliferation of mouse embryonic neural stem cells via the Notch
1044 signaling pathway. J Biol Chem *287*, 24356–24364. 10.1074/jbc.M112.365643.

1045 65.Kakuda, S., and Haltiwanger, R.S. (2017). Deciphering the Fringe-Mediated Notch Code:
1046 Identification of Activating and Inhibiting Sites Allowing Discrimination between Ligands.
1047 Dev Cell *40*, 193–201. 10.1016/j.devcel.2016.12.013.

1048 66.Stahl, M., Uemura, K., Ge, C., Shi, S., Tashima, Y., and Stanley, P. (2008). Roles of Pofut1
1049 and O-fucose in mammalian Notch signaling. J Biol Chem *283*, 13638–13651.
1050 10.1074/jbc.M802027200.

1051 67.Sun, X., Tie, H.C., Chen, B., and Lu, L. (2020). Glycans function as a Golgi export signal
1052 to promote the constitutive exocytic trafficking. J Biol Chem *295*, 14750–14762.
1053 10.1074/jbc.RA120.014476.

1054 68.Skrenkova, K., Lee, S., Lichnerova, K., Kaniakova, M., Hansikova, H., Zapotocky, M.,
1055 Suh, Y.H., and Horak, M. (2018). N-Glycosylation Regulates the Trafficking and Surface
1056 Mobility of GluN3A-Containing NMDA Receptors. Front Mol Neurosci *11*, 188.
1057 10.3389/fnmol.2018.00188.

1058 69.Janezic, E.M., Lauer, S.M.-L., Williams, R.G., Chungyoun, M., Lee, K.-S., Navaluna, E.,
1059 Lau, H.-T., Ong, S.-E., and Hague, C. (2020). N-glycosylation of α1D-adrenergic receptor
1060 N-terminal domain is required for correct trafficking, function, and biogenesis. Sci Rep *10*,
1061 7209. 10.1038/s41598-020-64102-4.

1062 70.Weis, W.I., and Drickamer, K. (1996). Structural basis of lectin-carbohydrate recognition.
1063 Annu Rev Biochem *65*, 441–473. 10.1146/annurev.bi.65.070196.002301.

1064 71.Zhao, Y., Sato, Y., Isaji, T., Fukuda, T., Matsumoto, A., Miyoshi, E., Gu, J., and Taniguchi,
1065 N. (2008). Branched N-glycans regulate the biological functions of integrins and cadherins.
1066 FEBS J *275*, 1939–1948. 10.1111/j.1742-4658.2008.06346.x.

1067 72.Yamamoto, K., Ito, S., Yasukawa, F., Konami, Y., and Matsumoto, N. (2005).
1068 Measurement of the carbohydrate-binding specificity of lectins by a multiplexed bead-based
1069 flow cytometric assay. Anal Biochem *336*, 28–38. 10.1016/j.ab.2004.09.030.

1070 73.Lee, T.K., Koh, A.S., Cui, Z., Pierce, R.H., and Ballatori, N. (2003). N-glycosylation
1071 controls functional activity of Oatp1, an organic anion transporter. Am J Physiol
1072 Gastrointest Liver Physiol *285*, G371-381. 10.1152/ajpgi.00358.2002.

1073 74.Ding, Y., Uchida, K., Aizawa, S.-I., Murphy, K., Berezuk, A., Khursigara, C.M., Chong,
1074 J.P.J., and Jarrell, K.F. (2015). Effects of N-glycosylation site removal in archaellins on the
1075 assembly and function of archaella in Methanococcus maripaludis. PLoS One *10*,
1076 e0116402. 10.1371/journal.pone.0116402.

1077 75.West, M.B., Wickham, S., Quinalty, L.M., Pavlovicz, R.E., Li, C., and Hanigan, M.H.
1078 (2011). Autocatalytic cleavage of human gamma-glutamyl transpeptidase is highly
1079 dependent on N-glycosylation at asparagine 95. J Biol Chem *286*, 28876–28888.
1080 10.1074/jbc.M111.248823.

1081 76.Hsiao, C.-C., Cheng, K.-F., Chen, H.-Y., Chou, Y.-H., Stacey, M., Chang, G.-W., and Lin,
1082 H.-H. (2009). Site-specific N-glycosylation regulates the GPS auto-proteolysis of CD97.
1083 FEBS Lett *583*, 3285–3290. 10.1016/j.febslet.2009.09.001.

1084 77.Branza-Nichita, N., Negroiu, G., Petrescu, A.J., Garman, E.F., Platt, F.M., Wormald, M.R.,
1085 Dwek, R.A., and Petrescu, S.M. (2000). Mutations at critical N-glycosylation sites reduce
1086 tyrosinase activity by altering folding and quality control. J Biol Chem *275*, 8169–8175.
1087 10.1074/jbc.275.11.8169.

78. Brack, A.S., Conboy, I.M., Conboy, M.J., Shen, J., and Rando, T.A. (2008). A temporal switch from notch to Wnt signaling in muscle stem cells is necessary for normal adult myogenesis. Cell Stem Cell *2*, 50–59. 10.1016/j.stem.2007.10.006.

79. Tanaka, S., Terada, K., and Nohno, T. (2011). Canonical Wnt signaling is involved in switching from cell proliferation to myogenic differentiation of mouse myoblast cells. J Mol Signal *6*, 12. 10.1186/1750-2187-6-12.

80. Hayward, P., Brennan, K., Sanders, P., Balayo, T., DasGupta, R., Perrimon, N., and Martinez Arias, A. (2005). Notch modulates Wnt signalling by associating with Armadillo/beta-catenin and regulating its transcriptional activity. Development *132*, 1819–1830. 10.1242/dev.01724.

81. Itakura, Y., Nakamura-Tsuruta, S., Kominami, J., Sharon, N., Kasai, K.-I., and Hirabayashi, J. (2007). Systematic comparison of oligosaccharide specificity of Ricinus communis agglutinin I and Erythrina lectins: a search by frontal affinity chromatography. J Biochem *142*, 459–469. 10.1093/jb/mvm153.

82. Delorme, E., Lorenzini, T., Giffin, J., Martin, F., Jacobsen, F., Boone, T., and Elliott, S. (1992). Role of glycosylation on the secretion and biological activity of erythropoietin. Biochemistry *31*, 9871–9876. 10.1021/bi00156a003.

83. Ishikawa, H., Uchida, T., Takahashi, S., Ishimori, K., and Morishima, I. (2001). Ligand migration in human myoglobin: steric effects of isoleucine 107(G8) on O(2) and CO binding. Biophys J *80*, 1507–1517. 10.1016/S0006-3495(01)76123-1.

84. van Berkel, P.H., van Veen, H.A., Geerts, M.E., de Boer, H.A., and Nuijens, J.H. (1996). Heterogeneity in utilization of N-glycosylation sites Asn624 and Asn138 in human lactoferrin: a study with glycosylation-site mutants. Biochem J *319 (Pt 1)*, 117–122. 10.1042/bj3190117.

85. Flack, M.R., Froehlich, J., Bennet, A.P., Anasti, J., and Nisula, B.C. (1994). Site-directed mutagenesis defines the individual roles of the glycosylation sites on follicle-stimulating hormone. J Biol Chem *269*, 14015–14020.

86. Jacob, G.S. (1995). Glycosylation inhibitors in biology and medicine. Curr Opin Struct Biol *5*, 605–611. 10.1016/0959-440x(95)80051-4.

Acknowledgments

Funding:

Irish Research Council (IRC) GOIPG/2016/1529 (EC)
Irish Research Council (IRC) GOIPG/2014/43 (MDL)
Government of Saudi Arabia ID: IR15208 (JG)
National Institutes of Health R01-AA024082 (EMR)
Science Foundation Ireland (SFI) award 11-PI-1128 (PAC)

Health Research Board (HRB), Ireland HRA-POR-2015-1315 (PAC)

Author contributions

Conceptualization: PAC, EC
Methodology: EC, AO, BOC, YG, RH, MDL
Investigation: EC, AO,
Visualization: EC, PAC
Supervision: PAC
Writing—original draft: EC, AO
Writing—review & editing: AO, EMR, PAC

Competing interests: Authors declare that they have no competing interests.

Data and materials availability: The datasets used and/or analysed during the current study are available from the corresponding author on reasonable request. All data are available in the main text or the supplementary materials.

Figures and Tables

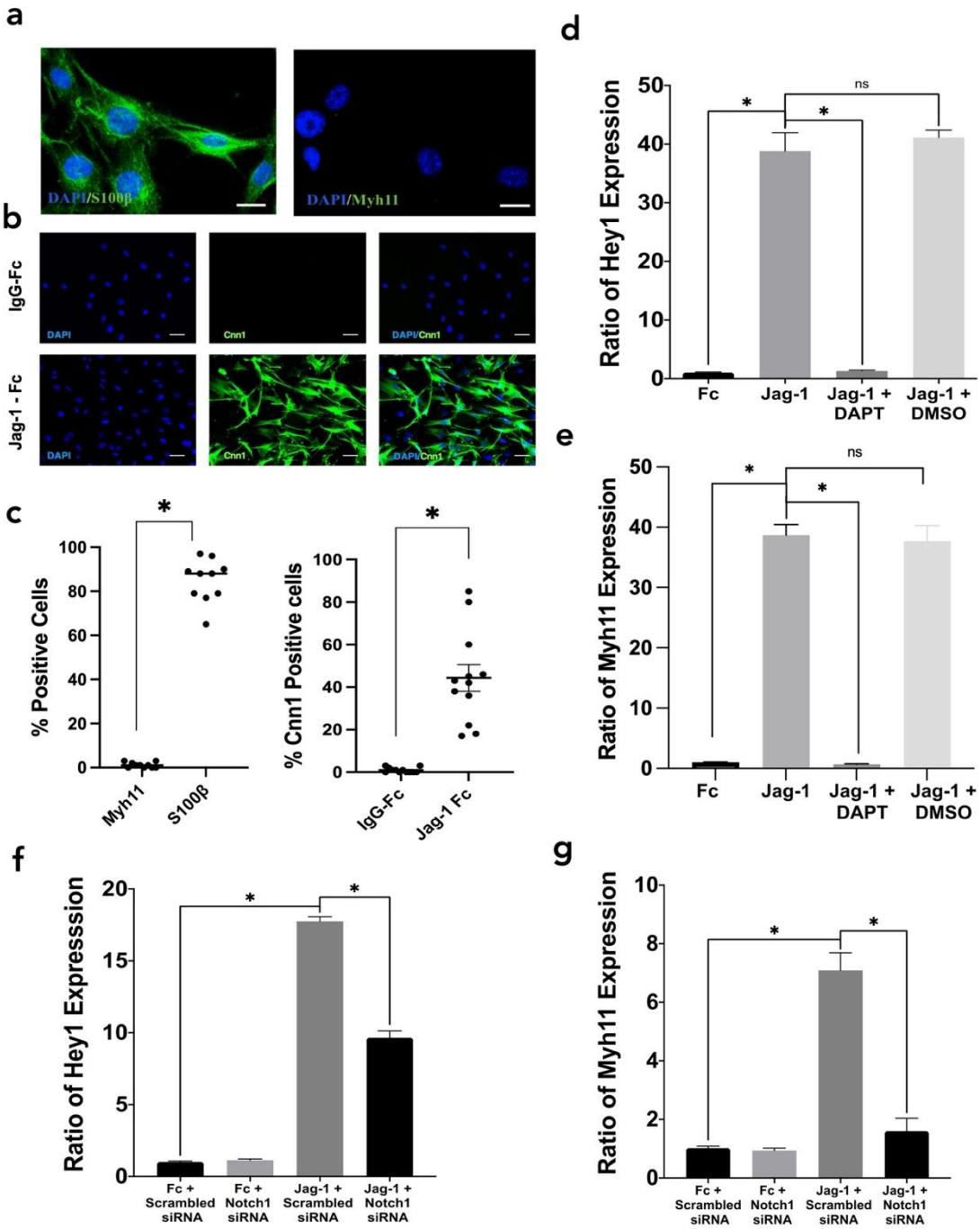

Figure 1: Jagged-1 activation of Notch1 signalling and SMC differentiation in S100β mVSCs. Immunocytochemical analysis of (a) Myh11 and S100β protein expression in untreated mVSCs and (b) Cnn1 expression in aortic S100β mVSCs treated with recombinant immobilised Jagged-1 (Jag-1 Fc) or IgG-Fc at 1μg/mL in MM1 media after 7 days. Scale bar = 25μm. (c) Mean percentage of Myh11, S100β and Cnn1 positive cells. DAPI was used to stain nuclei. Positive cells were counted and compared against total DAPI cell count. Data are the mean ± SEM and representative of n=3 *$p \leq 0.05$. (d-g) Real-time qRT-PCR analysis of *Hey1* and *Myh11* mRNA levels in S100β mVSCs treated with recombinant immobilised Jagged-1 (Jag-1 Fc) or IgG-Fc (Fc) at 1μg/mL for 48 hrs with or without prior treatment of cells with a γ-secretase inhibitor, DAPT versus DMSO control (d, e) and following Notch1 receptor knockdown (f-g) versus scrambled control. The gene, hypoxanthine phosphoribosyltransferase *(hprt*) was used as a housekeeping control. Data are the mean ± SEM and representative of n=3 *$p \leq 0.05$

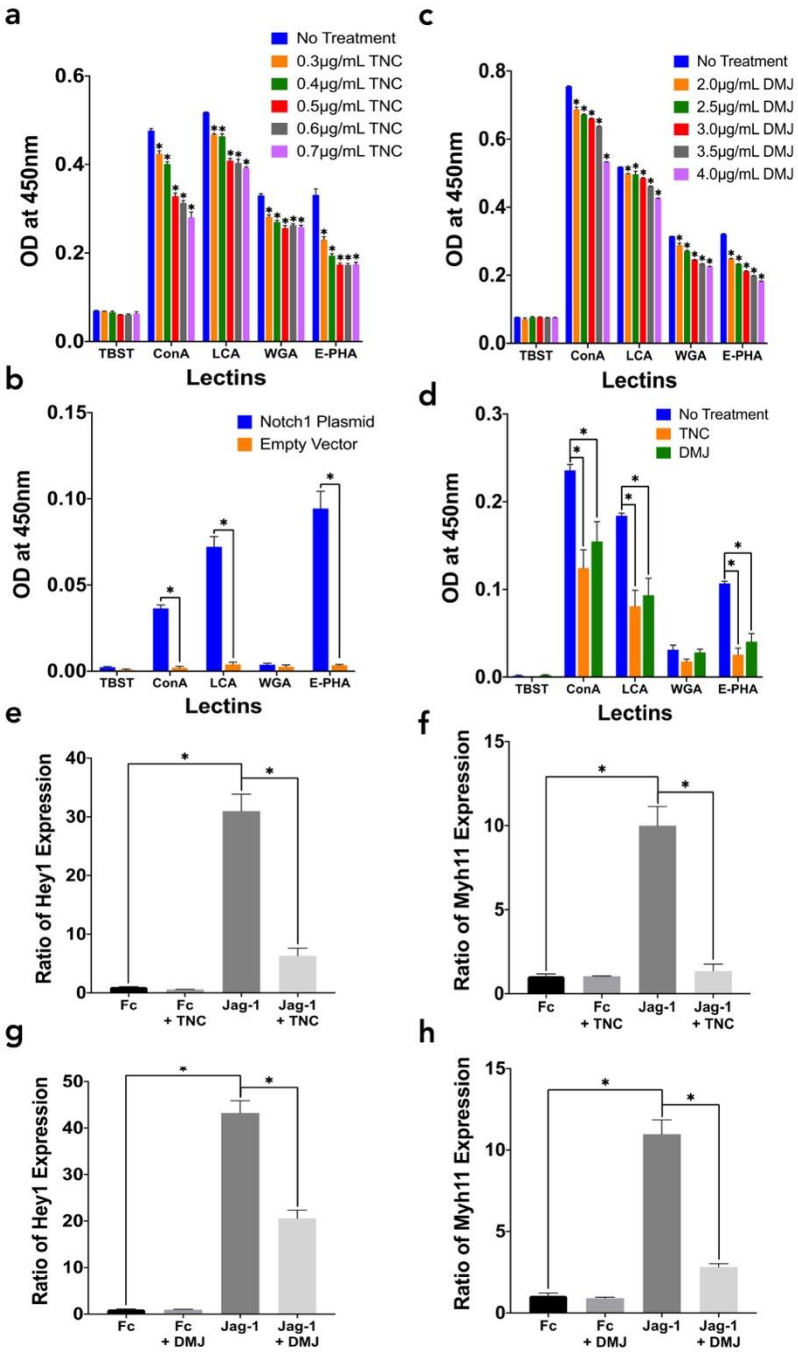

Figure 2: Chemical inhibition of N-glycosylation (TNC and DMJ) on lectin binding and Jagged-1 activation of Notch1 signalling and SMC differentiation in S100β mVSCs. ELLA analysis of N-glycan specific lectin binding of whole cell lysates (a, c) and immunoprecipitated ectopic expression of the Notch1 receptor (b, d) following treatment of S100β mVSC with a range of TNC (a, b) and DMJ (c, d) concentrations for 48 h at 37ºC. Data are presented as the mean absorbance value at 450 nm normalised to the negative control TBST sample. Data are the mean ± SEM and representative of n=3 *$p \leq 0.05$ compared to the non-treated sample probed with the same lectins. Real-time qRT-PCR analysis of *Hey1* and *Myh11* mRNA levels in S100β mVSCs treated with recombinant immobilised Jagged-1 (Jag-1 Fc) or IgG-Fc (Fc) at 1μg/mL in MM1 media after 48 hrs following ectopic expression of the Notch1 receptor with or without prior treatment of cells with TNC (0.5μg/mL) (e, f) and DMJ (4μg/mL) (g-h). The gene, hypoxanthine phosphoribosyltransferase *(hprt*) was used as a housekeeping control. Data are the mean ± SEM and representative of n=3 *$p \leq 0.05$

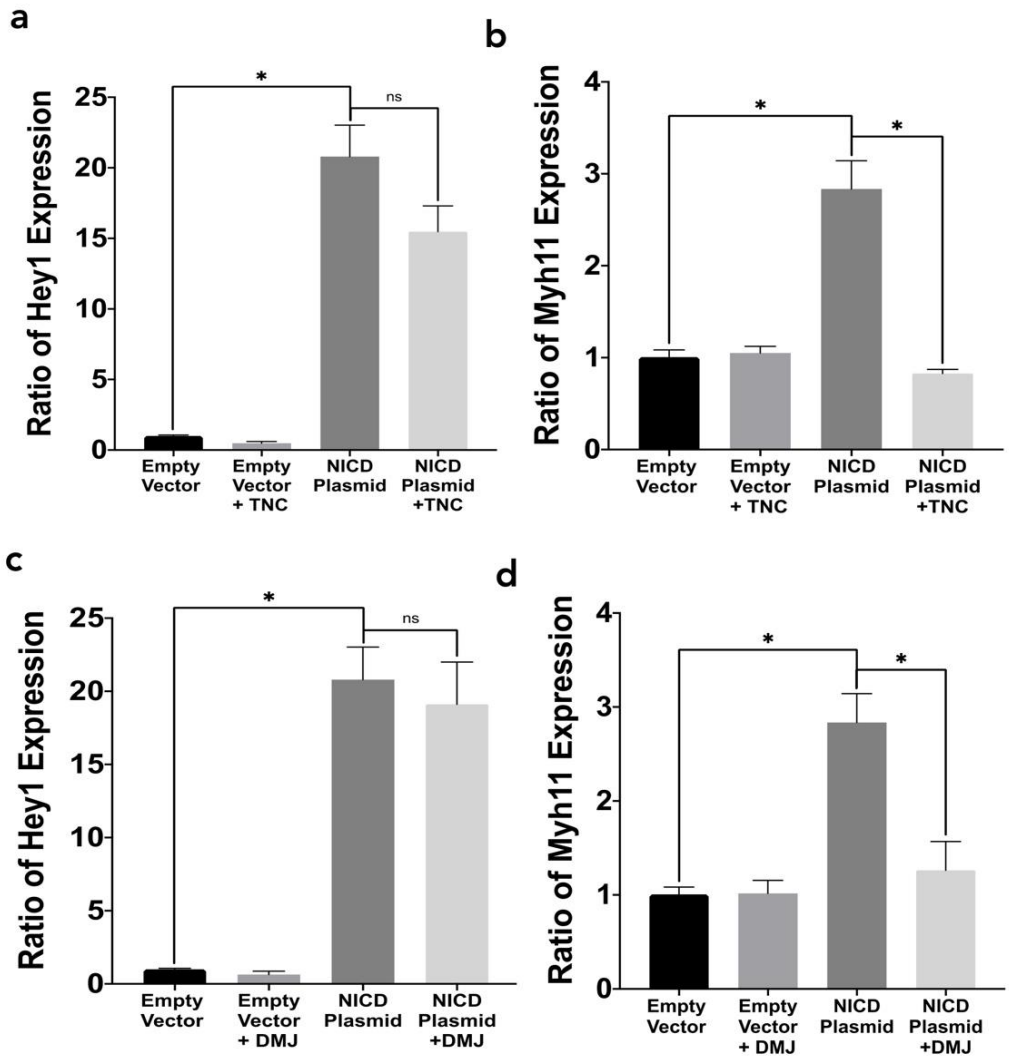

1185 **Figure 3**: **Chemical inhibition of N-glycosylation (TNC and DMJ) on Notch1 intracellular domain**
1186 **(NICD) activation of Notch signalling and SMC differentiation in S100β mVSCs**. Real-time qRT-PCR
1187 analysis of *Hey1* (a, c) and *Myh11* (b, d) mRNA levels in S100β mVSCs following ectopic expression of the
1188 Notch1 NICD after 48 hrs with or without prior treatment of cells with TNC (0.5µg/mL) (a, b) or DMJ
1189 (4µg/mL) (c-d). The gene, hypoxanthine phosphoribosyltransferase *(hpr*t) was used as a housekeeping
1190 control. Data are the mean ± SEM and representative of n=3 *$p \leq 0.05$.
1191
1192
1193
1194
1195
1196
1197
1198
1199
1200
1201
1202
1203
1204
1205

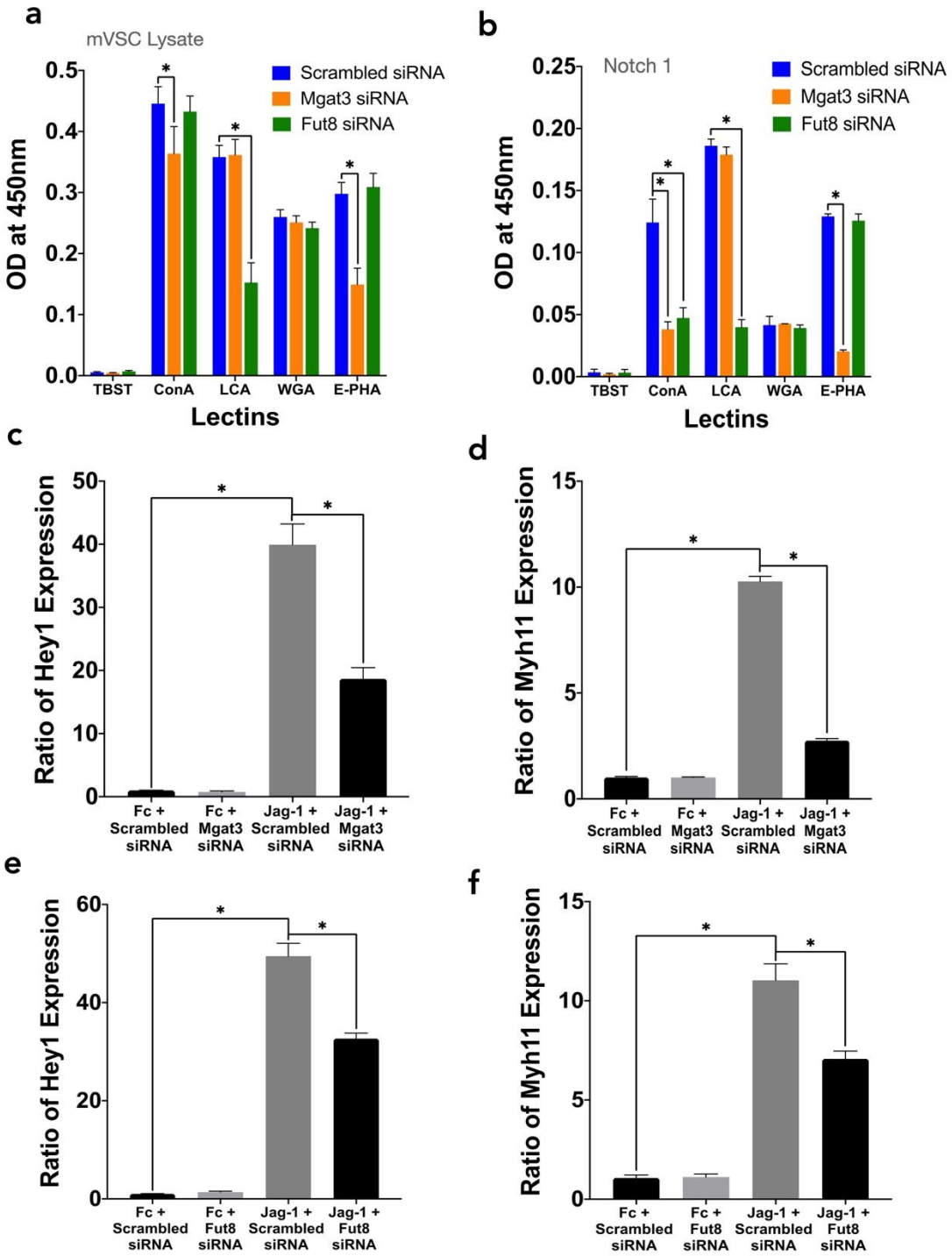

Figure 4: *Mgat3* and *Fut8* knockdown on lectin binding, Notch signalling, and SMC differentiation in S100β mVSCs. ELLA analysis of N-glycan specific lectin binding of whole cell lysate (a) and immunoprecipitated ectopic expression of the Notch1 receptor (b) following *Mgat3* and *Fut8* knockdown with specific siRNA duplexes (25nM) versus scrambled control. Data are presented as the mean absorbance value at 450 nm normalised to the negative control TBST sample. Data are the mean ± SEM and representative of n=3 *$p \leq 0.05$. compared to the non-treated sample probed with the same lectins. Real-time qRT-PCR analysis of *Hey1* (c, e) and *Myh11* (d, f) mRNA levels in S100β mVSCs treated with recombinant immobilised Jagged-1 (Jag-1 Fc) or IgG-Fc (Fc) at 1µg/mL after 48 hrs following *Mgat3* (c, d) or *Fut8* (e, f) knockdown with specific siRNA duplexes (25nM) versus scrambled control. The gene, hypoxanthine phosphoribosyltransferase *(hpr*t) was used as a housekeeping control. Data are the mean ± SEM and representative of n=3 *$p \leq 0.05$

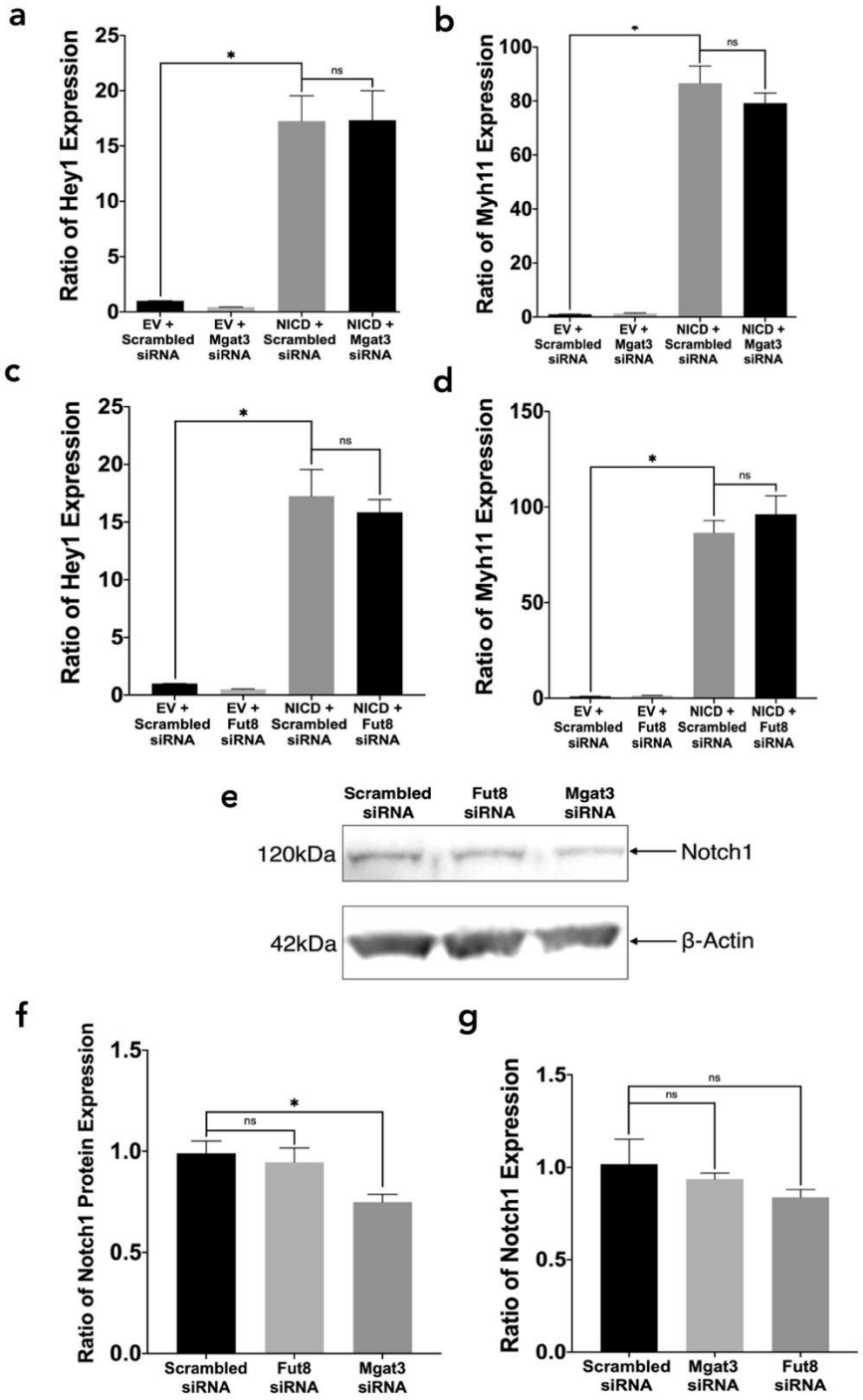

Figure 5: *Mgat3* and *Fut8* knockdown on Notch1 intracellular domain (NICD) activation of Notch signalling and SMC differentiation in S100β mVSCs. Real-time qRT-PCR analysis of *Hey1* (a, c) and *Myh11* (b, d) mRNA levels in S100β mVSCs stimulated by ectopic expression of Notch1 NICD after 48 hrs following *Mgat3* (a, b) and *Fut8* (c, d) knockdown with specific siRNA duplexes (25nM) versus scrambled control. The gene, hypoxanthine phosphoribosyltransferase *(hprt*) was used as a housekeeping control. Immunoblot analysis of Notch1 protein levels (e, f) and real-time qRT-PCR analysis of *Notch1* mRNA levels (g) following *Mgat3* or *Fut8* knockdown with specific siRNA duplexes (25nM) versus scrambled control. (e) a representative immunoblot image of Notch1 bands at 120kDa and β-actin bands at 42kDa. (f) Densitometry analysis of the intensity of Notch1 bands normalised to the β-actin loading control. Notch1 protein levels given as ratio of expression relative to the untreated negative control sample. (g) *Notch1* mRNA levels. Data are the mean ± SEM and representative of n=3, ns or *$p \leq 0.05$.

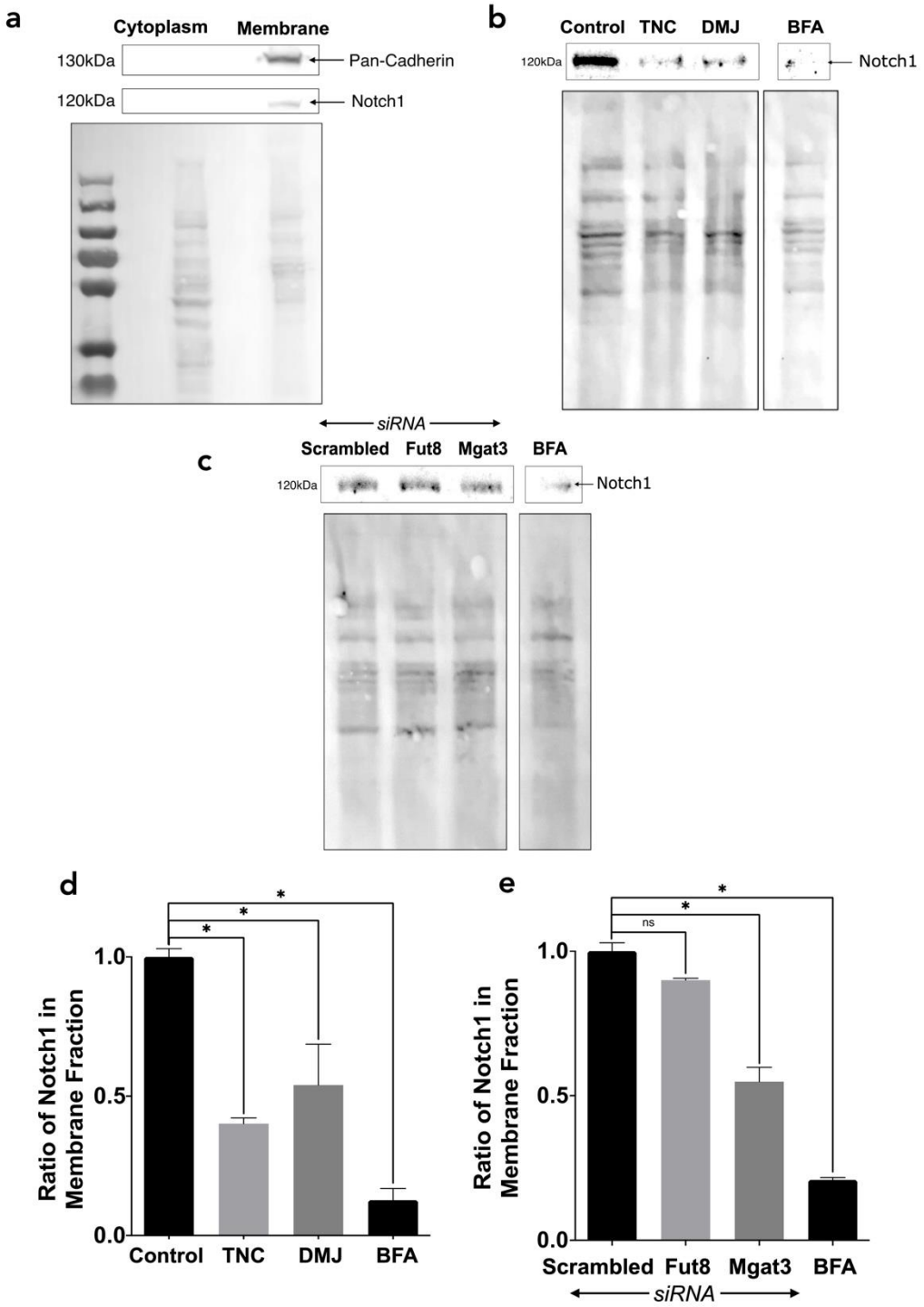

Figure 6: Chemical inhibition of N-glycosylation (TNC and DMJ) and *Mgat3* and *Fut8* knockdown on membrane localisation of the Notch1 receptor. (a) Membrane fractionation was carried out on S100β mVSCs lysates before Notch1 and Pan-Cadherin protein expression was assessed in cytoplasmic and membrane fractions, respectively. A representative immunoblot image of Notch1 at 120kDa (upper panel) and Ponceau S staining (lower panel) in each fraction. (b) Notch 1 protein expression in the membrane fractions of whole lysates from S100β mVSCs treated with TNC (0.5µg/mL), DMJ (4µg/mL) or 1 X BFA for 48 h at 37ºC. (c) Notch 1 protein expression in the membrane fraction of whole lysates from S100β mVSCs following *Mgat3* or *Fut8* knockdown compared to scrambled control or cells treated with 1 X BFA. (d, e) Densitometry analysis of the intensity of Notch1 bands normalised to the Ponceau S loading control. Notch1 protein levels in membrane fraction presented as the ratio of expression relative to the untreated negative control or scrambled control. Data are the mean ± SEM and representative of n=3, ns or *$p \leq 0.05$

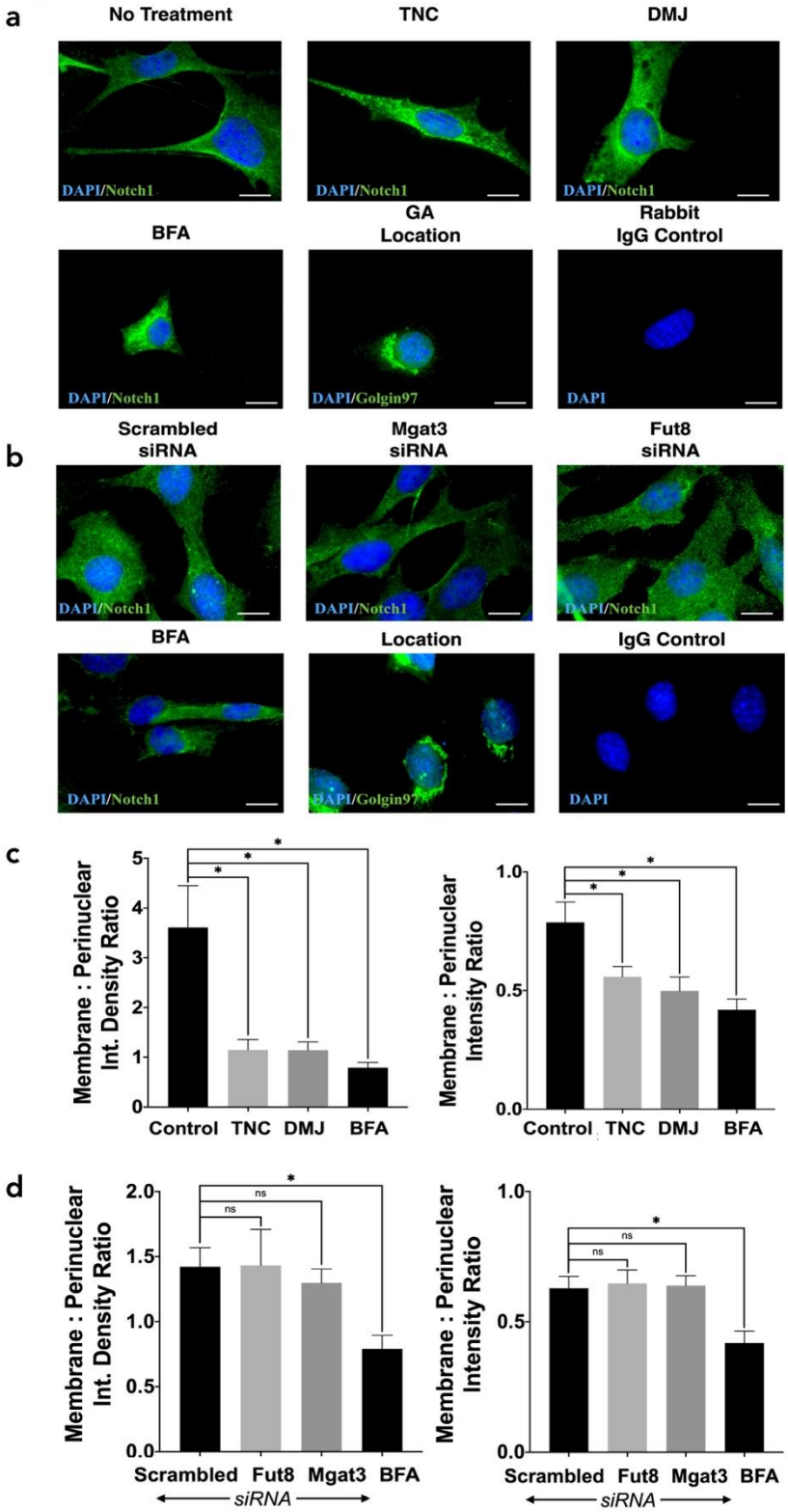

Figure 7: Chemical inhibition of N-glycosylation (TNC and DMJ) and *Mgat3* and *Fut8* knockdown on Notch1 receptor trafficking. Localization of Notch 1 receptor expression in S100β mVSCs treated with (a) TNC (0.5µg/mL), DMJ (4µg/mL) or 1 X BFA or (b) following *Mgat3* or *Fut8* knockdown, compared to untreated negative control sample, scrambled control, or treated with 1 X BFA for 48 h at 37ºC. Representative images at 60X magnification. Location of the GA was confirmed using Golgin-97. Scale bar = 10µm. (c-d) ImageJ used to calculate the ratio of Membrane: Perinuclear fluorescence using (c) integrated density and (d) mean fluorescence intensity values. Data are the mean ± SEM and representative of n=3, ns or *$p \leq 0.05$.

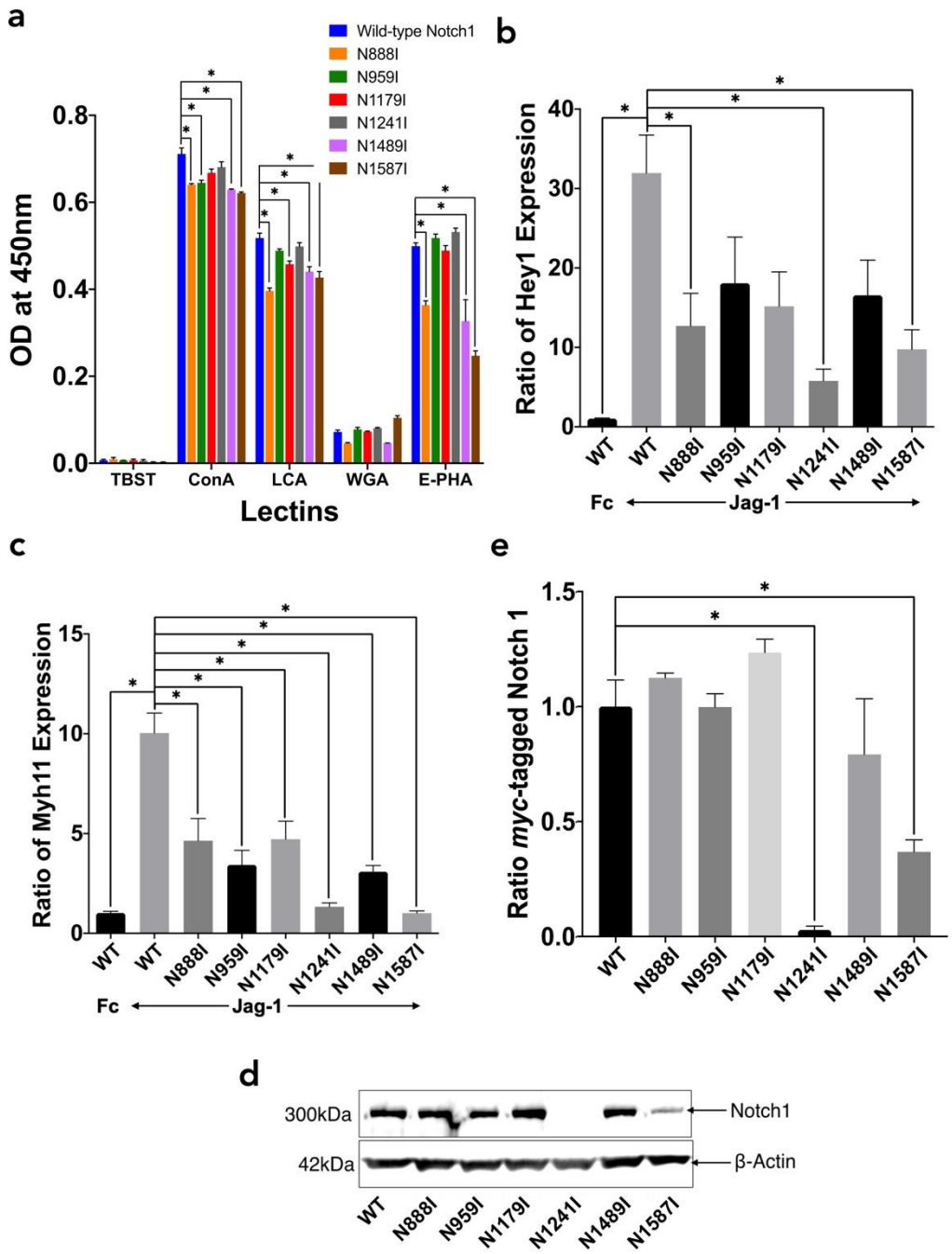

Figure 8: Site-directed mutagenesis of asparagine residues on the Notch1 ECD receptor on lectin binding, Notch signalling, and SMC differentiation in C3H10T1/2 cells. (a) ELLA analysis of N-glycan specific lectin binding of immunoprecipitated wild-type and mutant Notch1 receptors (N888I, N959I, N1179I, N1241I, N1489I and N1587I) from puromycin selected C3H10T1/2 cells. Data are presented as the mean absorbance value at 450nm normalised to the negative control TBST sample and the IgG immunoprecipitation control. (b, c) Real-time qRT-PCR analysis of Jag-1 stimulated *Hey1* (b) and *Myh11* (c) mRNA levels in C3H10T1/2 cells following ectopic expression of wild-type and mutant Notch1 receptors. Cells were treated with recombinant immobilised Jagged-1 (Jag-1 Fc) or IgG-Fc (Fc) at 1µg/mL in MM1 media after 48 hrs. The gene, hypoxanthine phosphoribosyltransferase *(hpr*t) was used as a housekeeping control. (d) Immunoprecipitated wildtype (WT) and mutant Notch1 receptor expression. A representative immunoblot image of full-length Notch1 bands at 300kDa and β-actin bands at 42kDa. (e) Densitometry analysis of the intensity of Notch1 bands normalised to the β-actin loading control. Full-length Notch1 protein levels presented as the ratio of expression relative to the wild-type Notch1 control. Data are the mean ± SEM and representative of n=3, ns or *$p \leq 0.05$.

Lectin	Binding specificity
ConA	Internal α-linked mannose
LCA	Internal α-linked mannose. Strongest affinity for mannose core with α-1,6 linked fucose bound to primary GlcNAc residue
WGA	High affinity for terminal GlcNAc and dimers/trimers of GlcNAc. Also reacts with chitobiose core of N-linked glycans, specifically the Man β(1,4)GlcNAc β(1,4)GlcNAc trisaccharide. Can also bind GlcNAc in O-glycans
E-PHA	Binds complex N-glycans. Usually at branching point from mannose core, specifically Galβ4GlcNAcβ2Manα6; (GlcNAcβ4); (GlcNAcβ4Manα3). Strong affinity for complex bisecting N-glycan structure.

Table I: The binding specificities of lectins. The binding specificity of Concanavalin A (ConA), Lens Culinaris Agglutinin (LCA), Wheat germ agglutinin (WGA) and Phaseolus vulgaris lectin E (E-PHA) on the ELLA assay.

Asn Site	N-Glycan Structures	Possible Role of Glycan
N888	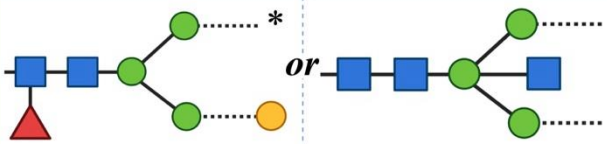	Regulation of receptor folding/cleavage
N959	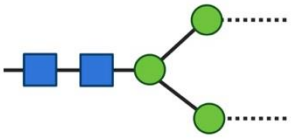	Impacts non-canonical Notch signalling
N1179	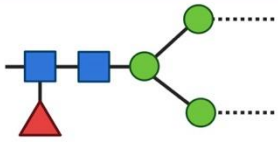	Impacts non-canonical Notch signalling
N1241	No N-glycan present 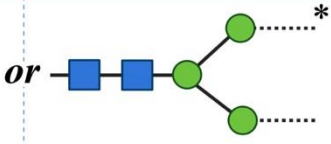	Regulation of receptor degradation
N1489	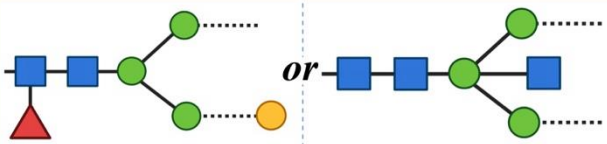	Impacts non-canonical Notch signalling
N1587	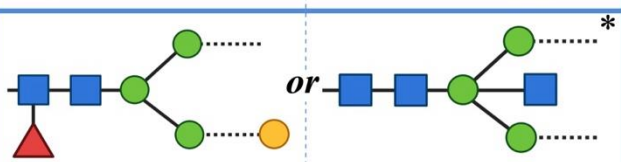	Regulation of receptor degradation

* Indicates most likely structure based on Notch1 expression and signalling data

Table II: N-Glycan Structures and Possible Roles on the Notch1 Receptor. The N-glycan structures and possible role of each glycan in regulating Notch signalling at specific asparagine residues on the Notch 1 ECD.